Phil. Trans. R. Soc. Lond. B. **268**, 23–38 (1974) [23]
Printed in Great Britain

The ultrastructure and chemistry of the luminal plasma membrane of the mammalian urinary bladder: a structure with low permeability to water and ions

By R. Marian Hicks, B. Ketterer and R. C. Warren
School of Pathology, Courtauld Institute of Biochemistry and Department of Physics as Applied to Medicine, Middlesex Hospital Medical School, London W1

[Plates 8–14]

The epithelium of the mammalian urinary bladder is an effective barrier to the free flux of urea, water and small charged ions between urine and tissue fluids. In this paper we present evidence to show that this permeability barrier passively depends on the structure of the unusual, thick, rigid membrane which limits the urinary surface of the epithelial cells.

The normal structure of this membrane is unique. Thickened plaques, composed of a hexagonal lattice of dodecameric subunits which extend through the depth of the membrane, are separated by thinner, unstructured, narrow bands. The regular structure of the lattice may be disrupted or distorted by treatment with urea, guanidine hydrochloride or sodium dodecyl sulphate.

Chemically the membrane is also remarkable. Its lipid component contains cerebroside, which apparently has an important effect in lowering water permeability. This effect is reinforced by cholesterol, which may be important for the maintenance of a condensed lipid layer during the mechanical stresses of bladder contraction and dilation. The protein component also is unusual in having a high proline content, and the significance of this is discussed in the context of membrane structure and function. At the moment it is not possible to relate the marked subunit structure of the membrane to its protein component although the large particle mass mucoprotein compound, as yet uncharacterized, may be located in the thick, densely staining, negatively charged surface lamina of the membrane.

This membrane is thus remarkable in both its structure and its function. These properties in turn must depend on complex interactions between its lipid and protein components which are themselves unusual.

Introduction

The mammalian urinary bladder is relatively impermeable to water and small charged ions (Johnson, Cavert, Lifson & Visscher 1951; Englund 1956; Levinsky & Berliner 1959; Rapoport, Nicholson & Yendt 1960; Kerr, Barkin, D'Aloisio & Menczyk 1963; Hicks 1966; McIntyre & Williams 1969). The barrier function depends on the integrity of the three cell thick epithelium which lines the bladder. Normally, the urine is hypertonic with respect to salts and urea when it enters the bladder, and despite the fact that the sub-epithelial capillaries are only a few micrometres away from the bladder lumen, the permeability barrier presented by the epithelium is such that the urine concentration remains almost constant (McIntyre & Williams 1969). There is a slow exchange of water molecules, urea and charged ions, but no net flux across the normal epithelium (Marucci *et al.* 1954). No other epithelium has yet been found which will satisfactorily substitute for the bladder epithelium as a permeability barrier between tissue fluids and urine, and the increased resorption of electrolytes and nitrogenous wastes through the mucosa of artificially constructed ileal or rectal bladders, with resultant hyperchloraemic acidosis and uraemia, has been a significant cause of morbidity and mortality in patients from whom diseased bladders have been removed (Marucci *et al.* 1954; Blandy 1964).

On investigating the basis of this blood/urine barrier, we concluded that two physical barriers existed in the bladder epithelium – an extracellular barrier located at the junctional complex

between the lateral membranes of the superficial cells near their luminal edge, and an intracellular barrier located at or in the membrane limiting the luminal face of the superficial cells (Hicks 1965).

Its barrier function appeared to be passive, and therefore by implication to depend on its physicochemical structure. If it were not so, much metabolic energy would be wasted in maintaining in the bladder the qualitative and quantitative differences between blood and urine achieved by the kidney. The facts that there is no obvious functional association of mitochondria with this membrane, and that unlike all other plasma membranes in the epithelium it has no nucleoside phosphatase activity (Hicks 1965, 1966), support the suggestion that it is a passive barrier. The development of a relatively water-proof bladder must have been an important evolutionary step for the early mammals in their adaptation from an aquatic existence to the harsh conditions of dry land. The very fact that this membrane is relatively impermeable to water makes it remarkable by comparison with other mammalian plasma membranes.

2. The structure of the bladder luminal membrane

The bladder luminal membrane is thicker than other plasma membranes, *ca.* 12 nm across, and has a prominent unit structure (Hicks 1965, 1966; Porter, Kenyon & Badenhausen 1967; Koss 1969). In the rat, the arrangement of hydrophilic and hydrophobic laminae is asymmetric, such that the outer hydrophilic lamina is approximately twice as thick as that on the cytoplasmic face of the membrane (Hicks 1965, 1966). Substructure can frequently be observed in these hydrophilic layers, and appears either as regular repeating densities in cross section (figure 1, plate 8) or as a hexagonal lattice in tangential sections of fixed, embedded material (Hicks 1965; Porter *et al.* 1967; Hicks & Ketterer 1970).

The membrane appears to have considerable physical rigidity and forms angular folds and ridges which give the surface of the luminal cells a characteristic angular appearance in profile (figure 2, plate 8). It is notable, that where there is a sharp bend in the membrane its asymmetry is lost and there is a thinner, flexible hinge-point (figure 1). This angular, rigid, luminal membrane is a feature of the mammalian urinary bladder, and in this laboratory we have observed it to be present in 16 different species including the desert-living gerbil, seals, a marsupial and man (Firth & Hicks 1971, 1973).

Examination of whole mounts of fresh or fixed membrane scrapings, confirm the observations made on fixed embedded material, and show this membrane to have a pronounced substructure (Hicks & Ketterer 1969).

The substructure is composed of subunits arranged in a regular hexagonal lattice and in most micrographs, each subunit appears by casual inspection to be subdivided into six smaller particles (figure 3, plate 9). The axis of each subunit is at an angle of 19° to the axis of the hexagonal lattice (Warren & Hicks 1970). This substructure is not unique to the rat, but has been observed in all mammalian species where it has been sought. Thus we have found it in the pig, calf, guinea pig, rabbit, hamster and man (Firth & Hicks 1973; Warren & Hicks 1971), Vergara, Longley & Robertson (1969) have reported it in the mouse and Staehelin, Chlapowski & Bonneville (1972) have also studied it in the rabbit.

This substructure is not uniform throughout the membrane, but appears as plaques when viewed from the surface, separated by the thinner, unstructured, hinge regions of the membrane (figure 4, plate 9). These plaques were first noted in sectioned membranes (Porter *et al.* 1967)

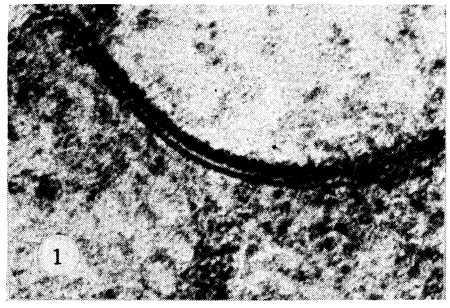

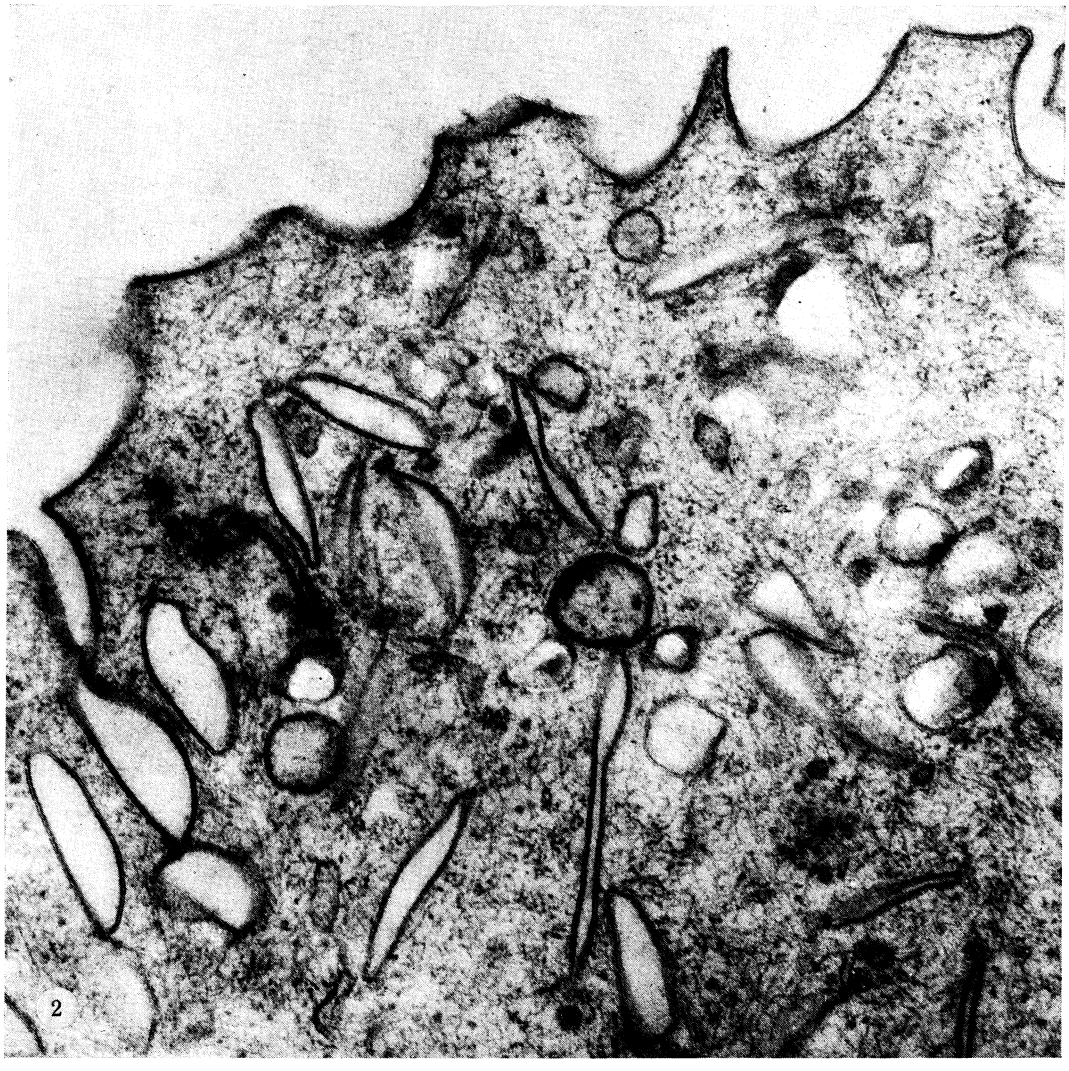

FIGURE 1. Cross-section of a portion of the cell membrane limiting a rat bladder epithelium superficial cell. Where the membrane is sharply bent it is about 8 nm thick and the two densely staining laminae are of about the same thickness. In the plaque region it is about 12 nm across, and the outer dense lamina adjacent to the urine is markedly thicker than that adjacent to the cytoplasm. Substructure is visible in the outer lamina. The tissue was fixed in phosphate-buffered osmium tetroxide and embedded in Epon and the thin section was contrast-stained with lead and uranyl salts. (Magn. × 200 000.)

FIGURE 2. Section of luminal cell cytoplasm in the rat bladder epithelium. The surface of the cell is limited by a rigid, angular membrane, with an easily resolved, trilaminate structure. This membrane also forms fusiform vacuoles in the cytoplasm. Tissue prepared as for figure 1. (Magn. × 60 000.)

(*Facing p.* 24)

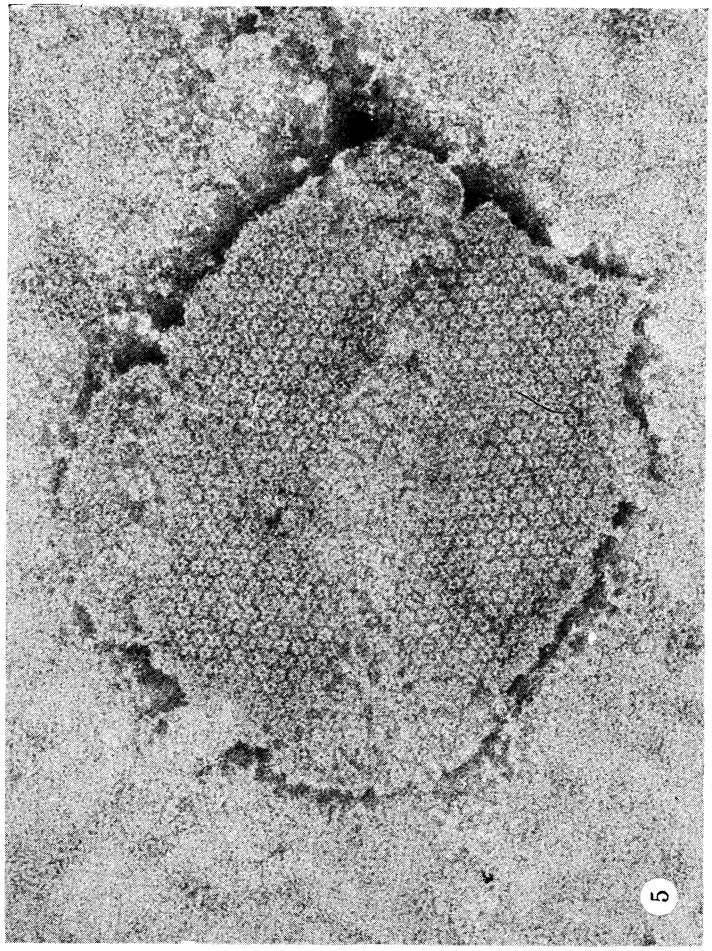

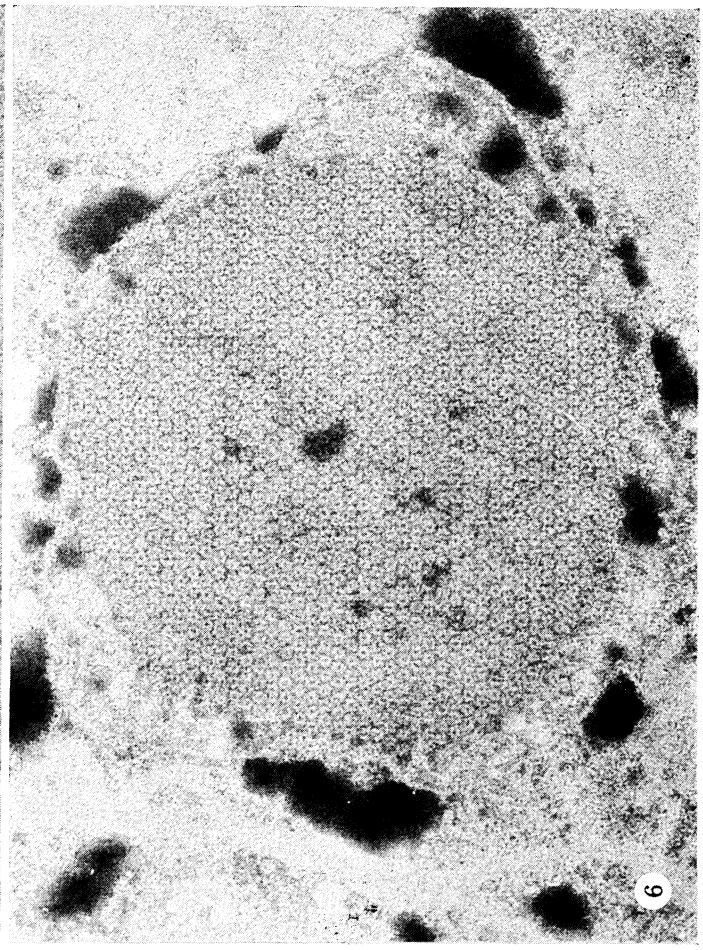

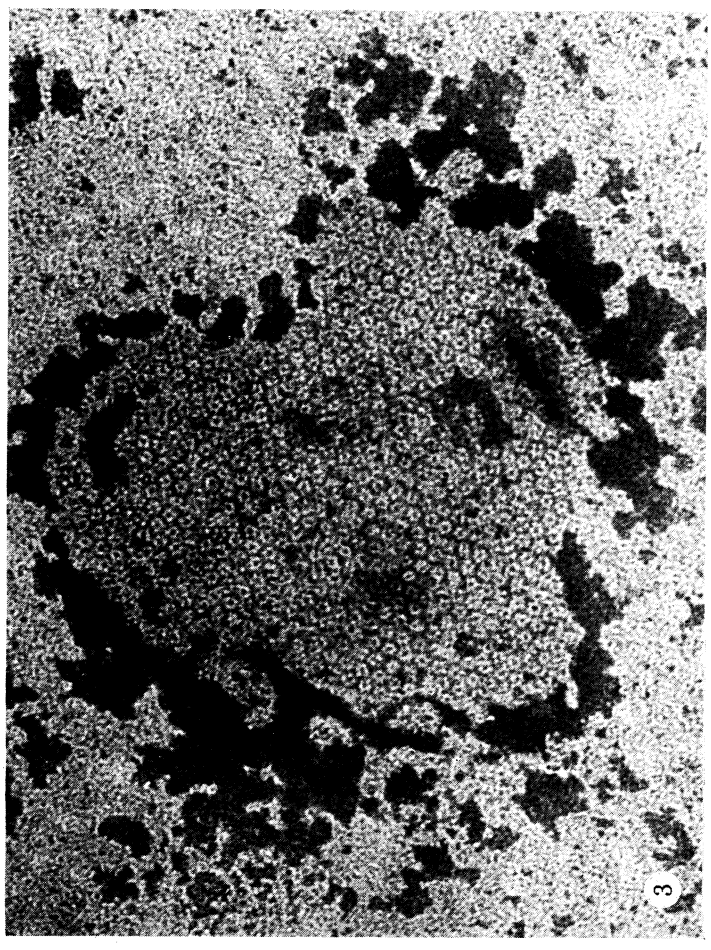

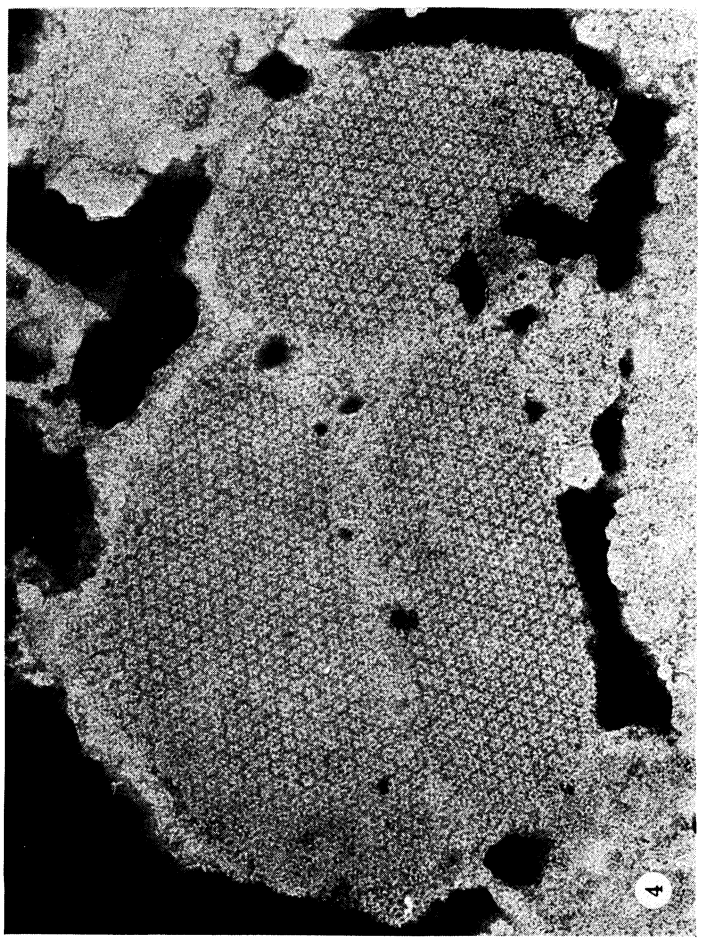

FIGURES 3 to 6. For description see opposite

and have now been clearly revealed not only by negative contrast staining as illustrated here, but also in freeze-fractured bladder luminal membrane (Staehelin *et al.* 1972).

Negatively stained preparations occasionally show pairs of plaques possessing approximate mirror symmetry (figure 5, plate 9). This could be expected if the membrane is assembled in the parallel cisternae of the Golgi complex, a process for which there is already strong evidence (Hicks 1966*b*), where it is possible that the two complementary faces of a cisterna may influence each other's symmetry. Each fusiform vesicle formed from a Golgi cisterna would then be expected to show mirror symmetry which would persist when the opened vesicle was inserted into the cell surface.

3. Substructure revealed by optical processing

The subunits contained within the hexagonal lattices are of such small dimensions that their substructure is masked by the granularity of the negative staining. However, since precise regularity of the arrangement may extend over large areas (figure 6, plate 9), the membrane is an ideal subject for the application of optical processing techniques in order to obtain the maximum amount of information from the image.

(*a*) *Linear integration*

Linear integration is a technique by which all the subunits in a given area are photographically superimposed, resulting in an average image in which the irregularities and granularities due to the staining process are greatly reduced (Markham, Hitchborn, Hills & Frey 1964). When the technique is applied to electron micrographs of the bladder luminal membrane, the subunits of the hexagonal array are found to consist of 12 particles each of approximate diameter 3 nm, arranged in a highly regular stellate configuration with the subunits skewed by 19° to the axes of the lattice (figure 7*a*, plate 10) (Warren & Hicks 1970). This regular dodecameric appearance may occasionally be observed in unprocessed images (figure 7*b*). Linear integration of electron micrographs possessing exceptionally high resolution sometimes reveals a small central particle, corresponding to the central spot visible in a number of subunits in the unprocessed images (figure 8, plate 10).

The remarkably high degree of symmetry of the averaged substructure is illustrated by a geometric model consisting of a 3 nm hexagonal lattice from which certain subunits have been omitted (figure 9) (Warren & Hicks 1971). Optical diffraction patterns of such an arrangement would show six very strong fifth-order diffraction spots, and diffraction patterns of high-resolution electron micrographs do in fact show these spots in precisely the predicted locations (figure 10).

Description of plate 9

Figure 3. A fragment of membrane from the surface of a human bladder, negatively stained with potassium phosphotungstate. The membrane is composed of a hexagonal lattice of subunits, each of which appears to be subdivided into six smaller particles. (Magn. × 150000.)

Figure 4. A piece of rat bladder surface membrane stained as in figure 3. The hexagonal lattice occupies three plaques which are separated by areas of membrane with no regular substructure. (Magn. × 150000.)

Figure 5. Negatively stained rat bladder luminal membrane, showing a pair of plaques possessing approximate mirror symmetry. Negatively stained with 2% potassium phosphotungstate, pH 7.2 (Magn. × 160000.)

Figure 6. Large plaque, stained as for figure 5. (Magn. × 142000.)

(b) Optical filtering

Optical filtering of the diffraction pattern (Klug & DeRosier 1966) to remove unwanted granularity and reconstruct a noise-free image gives the result shown in figure 11, plate 11. This form of processing does produce a certain amount of averaging of the subunits (Fraser & Millward 1970), but this may be kept to a minimum, as opposed to the maximal averaging of

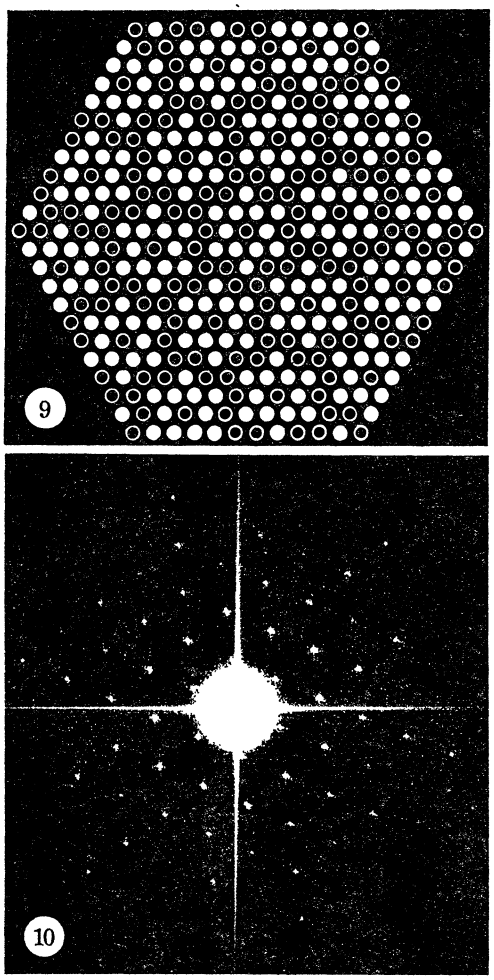

FIGURE 9. Model of the membrane lattice based on a 3 nm hexagonal lattice of particles. The white disks represent the particles visible in the processed images, while the open circles fill the spaces between them. The dodecamers may be seen more clearly by viewing from a distance or with the eyes defocused.

FIGURE 10. Optical diffraction pattern of the negative of figure 6. Four hexagonal rings of spots are visible at a spacing corresponding to the 14 nm repeat unit. Of the fifth-order spots, only the six corresponding to the 3 nm lattice of figure 9 are visible.

the linear integration technique. As a result, filtered images do not usually show such a precisely stellate configuration, but instead the position and shape of its constituent particles show some variation (figure 12, plate 11). In general, these variations average out during linear integration, to produce the regular stellate configuration illustrated in figure 7. Occasionally, however, regions of membrane may be observed which when integrated show the presence of a predominant variation (figure 13, plate 11).

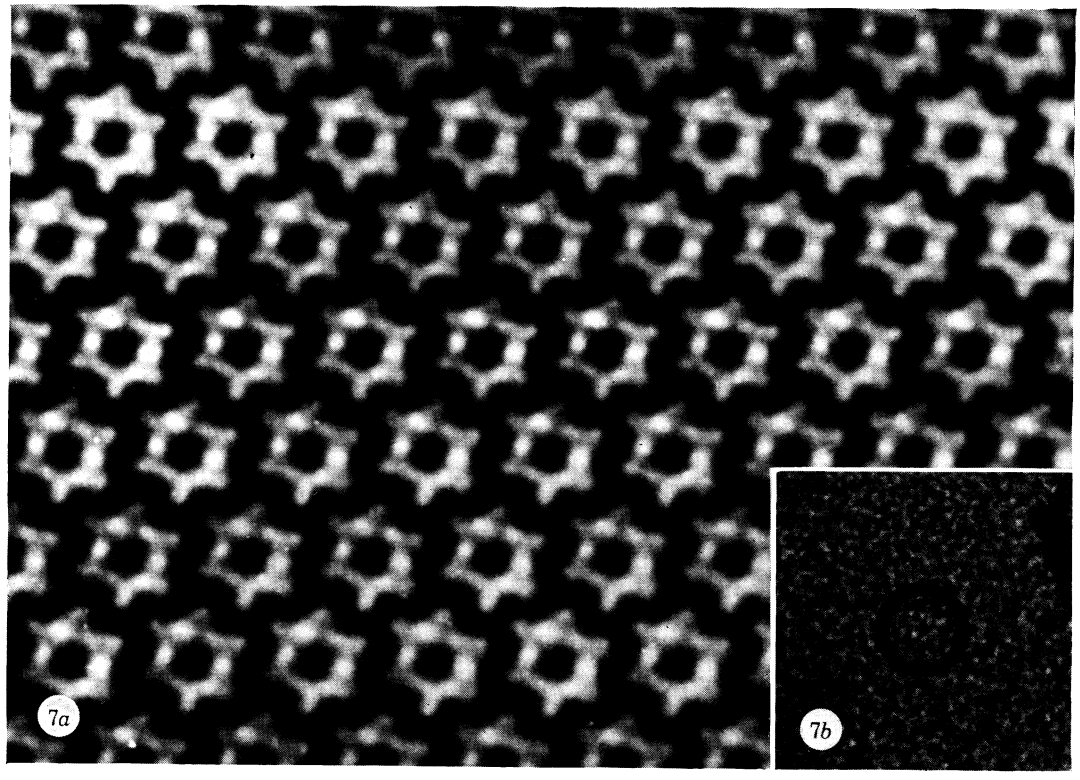

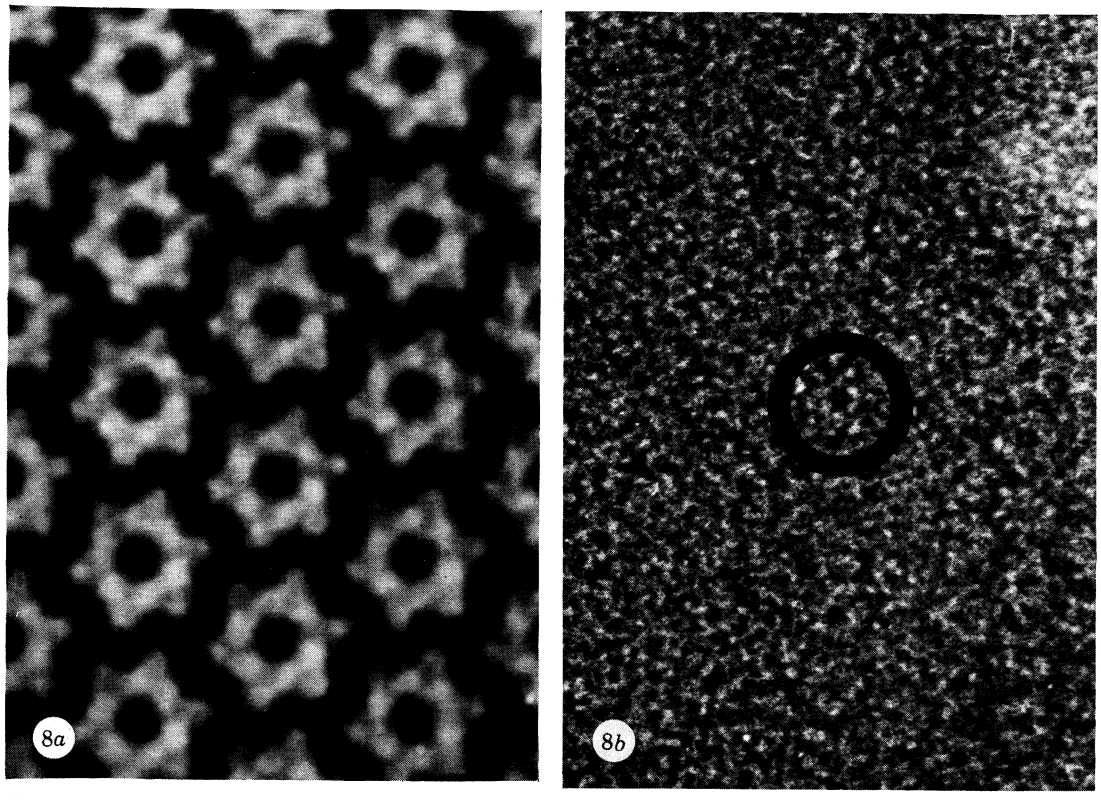

FIGURE 7. (*a*) Negatively stained rat bladder luminal membrane, processed by linear integration. Each subunit is composed of 12 particles of diameter 3 nm, and is skewed by 19° to the axis of the lattice. (Magn. × 1 100 000.) (*b*) Unprocessed image showing central particles. (Magn. × 440 000.)

FIGURE 8. (*a*) Integrated image showing central particles (Magn. × 1 600 000). (*b*) Unprocessed image showing central particle (Magn. × 680 000).

(*Facing p.* 26)

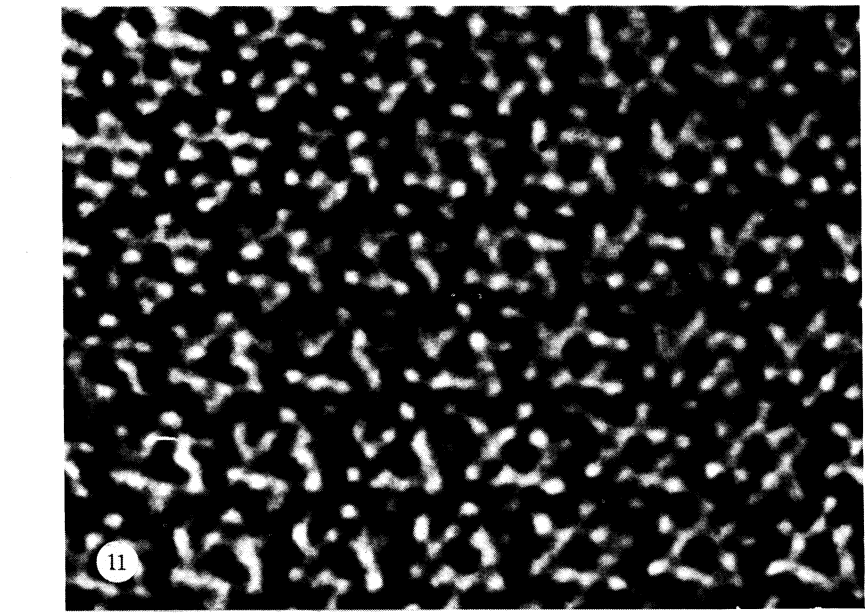

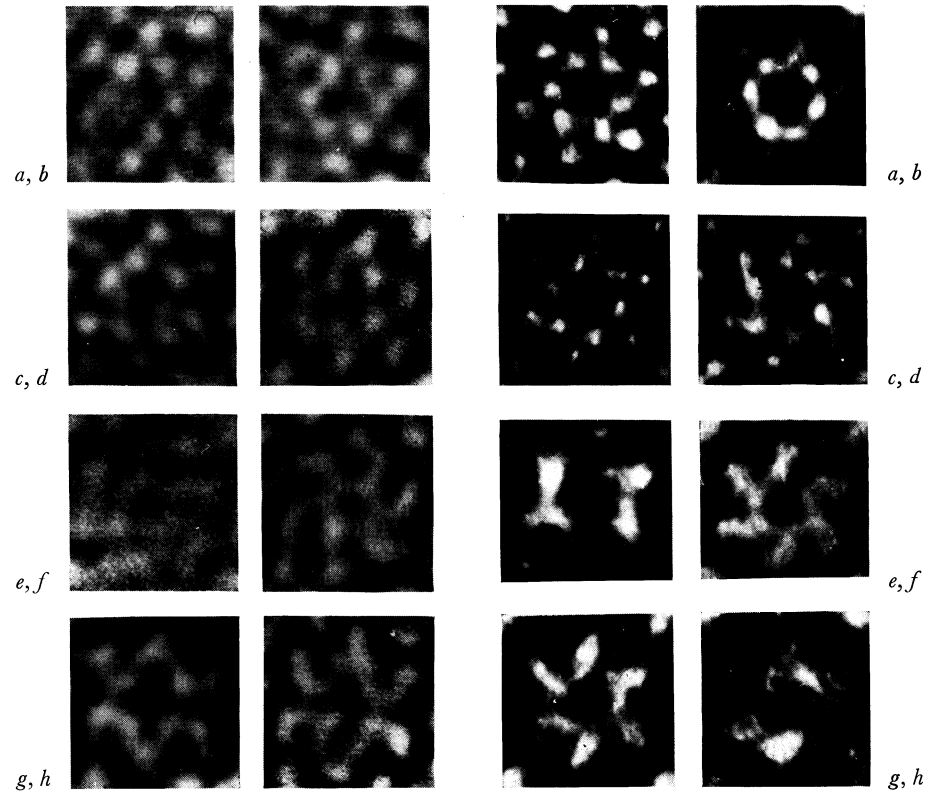

FIGURE 11. Optically filtered image of rat bladder luminal membrane. (Magn. × 1 100 000.)

FIGURE 12. Optically filtered subunits showing various configurations. Taken from rat (*a*, *b*, *e* and *g*) and calf (*c*, *d*, *f* and *h*). The subunit shown in (*e*) is taken from a bladder exposed to urea, and (*g*) is from a bladder exposed to sodium dodecyl sulphate (SDS). (Magn. × 1 700 000.)

FIGURE 13. Integrated subunits, showing variations which occasionally appear after averaging over a large number of subunits. Taken from rat (*b*, *e*, *g* and *h*) and calf (*a*, *c*, *d* and *f*); (*g*) has been exposed to SDS. (Magn. × 1 700 000.)

(*c*) *Three-dimensional structure*

Staehelin *et al.* (1972) have shown by freeze-fracture studies that the subunits penetrate almost the whole width of the membrane, and are not confined solely to the outer surface. Further evidence to support this finding comes from studies of sections of fixed and embedded material.

In well-preserved specimens, tangential sections may show hexagonal arrays of dots while transverse sections cut in a favourable orientation show bi-layers consisting of rows of elongated subunits (figure 14, plate 12) (Chlapowski, Bonneville & Staehelin 1972). The subunits have a mean centre-to-centre separation of 12 to 13 nm, and are usually seen in the thickened outer dense lamina, although they have also been observed in the inner, cytoplasmic dense lamina. This appearance has been observed in electron micrographs taken from a number of different mammals using a variety of fixatives. Portions of membrane were selected for linear integration analysis, with the results shown in figure 14. The subunit appearance is preserved to a different extent in each membrane, but is notably more prominent in the thicker luminal dense lamina. The clear central lamina, which has a mean thickness of 3 nm, is also prominent in most membranes analysed. It is therefore apparent that only the extremities of the subunits are hydrophilic and capable of taking up stain, while their central regions and the spaces between them are generally hydrophobic and are not stained.

Negative stains, unlike the positive stains illustrated in figure 14, form an electron-dense lake surrounding the membrane and give information concerning its surface topography. The depth of the subunits observed by negative staining may be indicated by studying tilted membranes. Experiments in which the membrane was tilted by up to $\pm 30°$ revealed no significant alteration in the appearance of the subunits. However, membranes lying on an uneven surface were occasionally observed to be tilted to greater angles and measurement of the apparent subunit spacing enabled the angle of tilt to be calculated. Although such membranes were too curved to allow optical analysis to be performed, the central dark hole and the dark regions between the subunits could still be discerned at tilt angles of up to 60° (figure 15, plate 12). From this it can be calculated that the subunits project from the matrix of the membrane by no more than 3 nm.

(*d*) *Substructural changes induced by chemical treatment of the membrane*

Some samples of membranes were examined after the luminal surface of the bladder had been exposed to chemical agents. 1.5 M guanidine hydrochloride, 2 M urea or 1% sodium dodecyl sulphate (SDS) appear to increase the degree of variation of the subunits from the regular stellate appearance (figures, 12, 13, plate 11 and 16*a*, *b*, plate 12). Exposure to SDS, in addition to increasing the variability of the substructure, appears to permit mobility of the subunits, which become displaced from the regular lattice and either aggregate (figure 17, plate 12) or, more occasionally separate (figure 15, plate 12).

4. The permeability of the bladder luminal membrane

(*a*) *Permeability of normal membrane*

As explained above, the permeability barrier between tissue fluids and urine depends on the integrity of the luminal membrane plus the junctional complex between superficial cells in the bladder epithelium. An assessment of the permeability of the bladder epithelium can be made

by measuring the net electrolyte flux across the bladder. We have done this both *in vivo* and *in vitro* by instilling a known quantity of lithium ions into the bladder lumen and measuring the rate at which the lithium was lost from the bladder *in vivo*, or appeared in stirred Ringer solution surrounding the ligated bladder *in vitro*. Lithium analyses were made by Mr R. L. Warren, Courtauld Institute of Biochemistry, by emission flame spectrophotometry (see Warren 1959 for method).

The rate at which lithium crossed the bladder wall was found to be linear for the first 3 h.

The permeability constant for lithium was calculated from the formula

$$K = \frac{V}{AT} \ln \left(\frac{C_1 - C_0}{C_1 - C_0 \text{ at time } T} \right),$$

where V is the volume of solution in bladder, A the area of membrane lining the bladder, C_1 the concentration of lithium inside the bladder, and C_0 the concentration of lithium outside the bladder.

The above formula is valid only if C_1 is so much in excess of C_0 that it remains effectively unchanged over time T.

Because of the folding of the luminal surface it is not possible to estimate accurately the surface area of the epithelium in contact with lithium solution in the bladder lumen. As a first approximation, it has been assumed that a bladder containing 0.4 ml fluid, which is sufficient to give a moderate distension, has a surface area of 3 cm^2. Using this value, the approximate permeability constant for lithium across the normal rat bladder *in vitro* is 1.1×10^{-6} cm s^{-1}.

No attempt has been made to calculate the permeability constants for the *in vivo* experiments, because both the volume of the bladder and the surface area of the epithelium change during the course of the experiment as fresh urine enters and distends the bladder from the ureters. Furthermore, the concentration of lithium in the bladder decreases, not only by loss across the epithelium, but also by dilution with urine. However, the total amount of lithium in the bladder at the beginning and end of the experiment can be estimated from the volume and lithium concentration measurements, and then the total loss across the epithelium estimated. For comparison, the lithium flux is expressed both for *in vivo* and *in vitro* experiments as a diffusion rate, in mmol lithium leaving the bladder per minute and also as the percentage of the original total passing out of the bladder per minute. Comparison of the *in vivo* and *in vitro* values show that, despite the variables and approximations, the diffusion rate can be used as a rough index of

---

Description of plate 12

Figure 14. Sections of bladder luminal membrane showing subunit appearance (below) and their images after linear integration (above). Taken from pig (*a* and *b*) and mouse (*c*, *d* and *e*), fixed with osmium tetroxide, and hamster (*f*) fixed with glutaraldehyde. In (*g*), nine integrated images have been superimposed, and the same nine images reversed, to give a symmetrical average image. (*a* to *f*, magn. × 310 000; (*g*) magn. × 620 000.)

Figure 15. Negatively stained rat bladder luminal membrane after exposure to SDS. The membrane is lying on an uneven substrate and is tilted to a maximum of 60°. Isolated subunits may be observed near the centre. (Magn. × 185 000.)

Figure 16. (*a*) Negatively stained rat bladder luminal membrane after exposure to guanidine hydrochloride. Magn. (× 160 000.) (*b*) Image of (*a*) after linear integration, to reveal an average structure similar to figure 13*e*. The resolution is not sufficient for 12 particles to be distinguished. (Magn. × 700 000.)

Figure 17. Negatively stained rat bladder luminal membrane after exposure to SDS. Aggregation of the subunits is apparent in the right half of the picture. (Magn. × 250 000.)

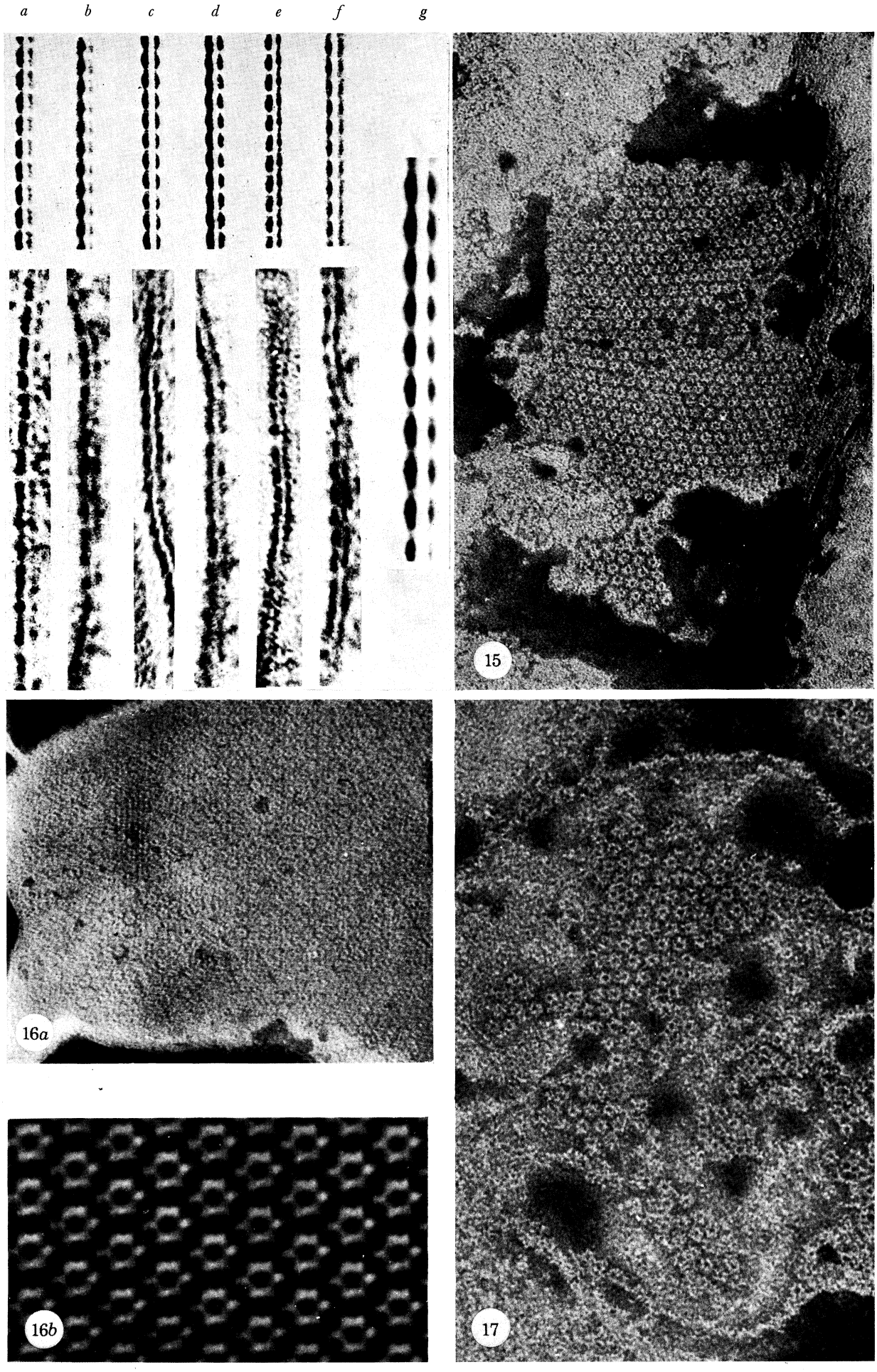

FIGURES 14–17. For description see opposite

(*Facing p.* 28)

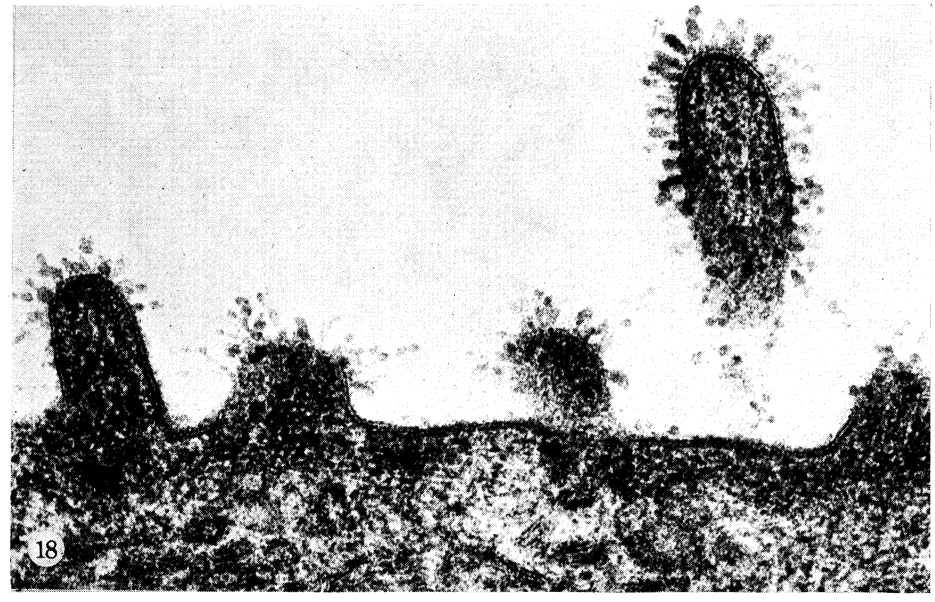

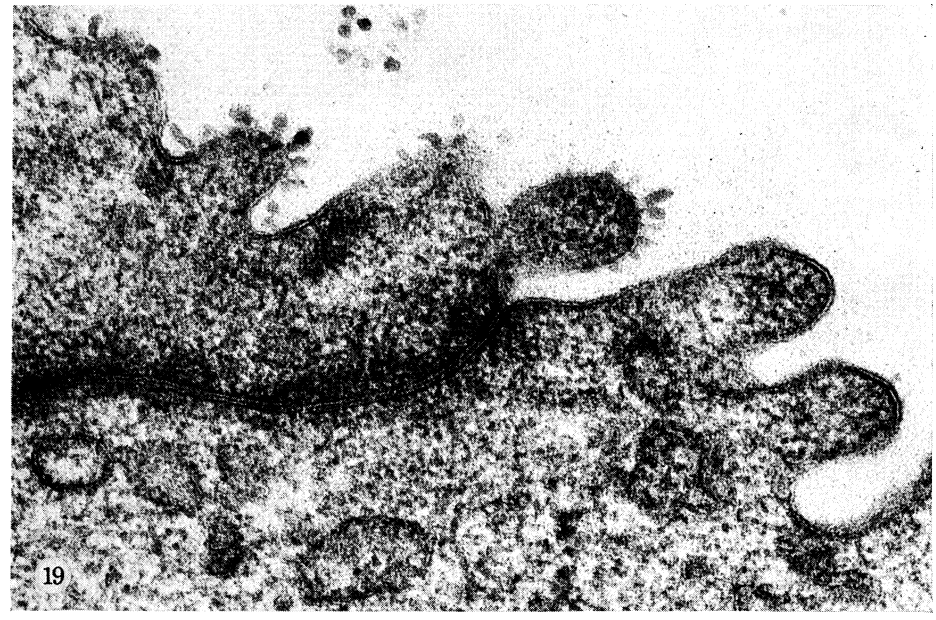

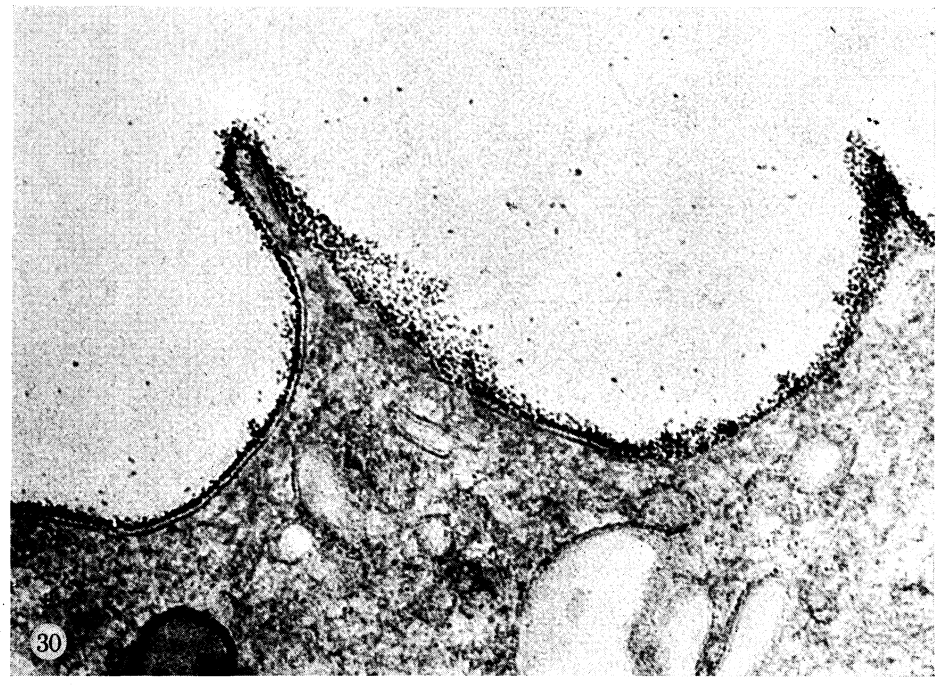

FIGURES 18–19 and 30. For description see opposite

the permeability of the bladder to lithium. The lithium flux is very low across the bladder by comparison with the flux across a dialysis tube containing the same amounts of lithium in the same volume (table 1).

(*b*) *Permeability of bladders with a modified luminal surface membrane*

During carcinogenesis in the bladder epithelium, structural changes occur in the luminal surface membrane. In animals where carcinogenesis has been induced by dibutyl nitrosamine, DBN, the superficial cells gradually de-differentiate and eventually the normal luminal membrane with its highly ordered substructure is replaced by a thinner, more flexible membrane which has a pronounced filamentous surface coat (figure 18, plate 13). This modified membrane has no hexagonal substructure when inspected after negative contrast staining.

TABLE 1. LITHIUM FLUX

	%/min	mmol/min
(*A*) Across a rat bladder		
in vivo	0–0.01	$0–2.3 \times 10^{-6}$
in vitro	0–0.01	$0–3.3 \times 10^{-6}$
(*B*) Across a dialysis sac		
	1.6	4.0×10^{-4}

0.4 ml of tissue culture medium containing 0.01 mmol/l of lithium was instilled into either the bladder or the dialysic sac. The amount of lithium remaining in the bladder or sac after 2½ h was estimated (Warren 1959). In addition, for *in vitro* bladders and dialysis sacs, where they were suspended in 10 ml stirred, oxygenated tissue culture medium at 37 °C, micro-samples of the bathing medium were analysed at half-hourly intervals for lithium.

For the first 20 to 30 weeks the tight junctions between the superficial cells remain morphologically normal and the number of superficial cells becoming transformed and losing their normal specialized surface membrane increases. The lithium flux across the bladder also rises steadily (figure 20). Later, as the tumours become more disorganized, the junctional complexes between cells also decrease in number.

Similar results have been obtained with another bladder carcinogen, methylnitrosourea, MNU. At first there is cell death, and partial stripping of the epithelium, so that both barriers, membrane and junctional complex, fail. This is associated with a very high flux of lithium across the bladder after each dose of MNU (figure 21). The normal epithelium is replaced by many layers of de-differentiated cells and is limited on the luminal face, as after DBN treatment, by a thin, flexible membrane with a superficial filamentous coat. The lateral borders of the

---

DESCRIPTION OF PLATE 13

FIGURE 18. The luminal cell membrane from the bladder of a rat 16 weeks after commencing treatment with the bladder carcinogen, dibutylnitrosamine. The membrane has lost its rigidity and also its unusual structural differentiation. It no longer has thickened plaques with a highly ordered substructure, but instead is about 7.5 nm thick, with a filamentous surface coat. (Magn. × 90000.)

FIGURE 19. Part of two superficial cells from the bladder epithelium of a rat 6 weeks after starting treatment with methylnitrosourea. The cells are joined along their lateral borders by a pentalaminate tight junction. The cell surfaces are limited by a flexible 7.5 nm thick membrane covered by a filamentous surface coat, but there are no rigid, structural plaques such as are seen in the normal animal. (Magn. × 100000.)

FIGURE 30. Uptake of colloidal iron from acid solution by the bladder luminal membrane. The iron is adsorbed to the external surface of the membrane, indicating that the membrane has a strong negative charge. (Magn. × 100000.)

superficial cells in this de-differentiated epithelium are again joined by junctional complexes (figure 19, plate 13), but the flux of lithium across the epithelium remains high, (figure 21). In some of these MNU-treated animals the permeability constant, measured *in vitro*, rises to 1.1×10^{-4} cm s^{-1} at 20 weeks by comparison with 1.1×10^{-6} cm s^{-1} for normal control animals.

These experiments suggest that the highly organized substructure of the normal luminal surface membrane may well be responsible for the low permeability of the normal bladder. When this organization is lost, as it is from the surface membrane of the DBN- and MNU-transformed bladder epithelium, the lithium flux across the bladder is greatly increased.

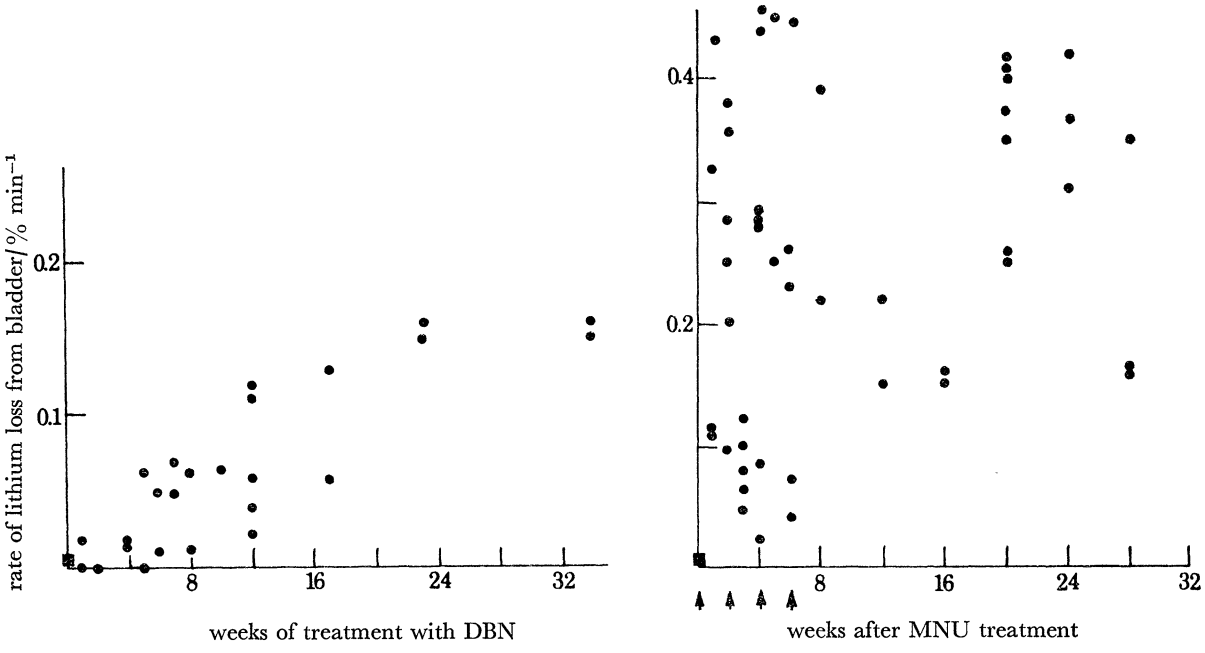

FIGURE 20. Lithium flux across rat bladders after treatment of the animals with dibutylnitrosamine (DBN). Each point was obtained with a different rat. The square near the origin of the ordinate shows the average lithium flux across the bladders of ten normal rats.

FIGURE 21. Lithium flux across rat bladders after treatment with up to four doses (indicated by pointers) of methylnitrosourea (MNU). Each point represents the value for a single animal. The square on the ordinate is the average flux across ten normal rat bladders.

5. Isolation and chemical analysis of the bladder luminal plasma membrane

It is reasonable to assume that the structure and low permeability of this membrane are determined by its molecular organization. As a first step towards understanding this, the membrane has been isolated (Hicks & Ketterer 1970) and some chemical analyses have been performed upon it (Ketterer, Hicks, Christodoulides & Beale 1973).

(*a*) *Isolation*

A successful preparation of the membrane was obtained by flooding the bladder lumen with fluorescein mercuric acetate (Warren, Glick & Nass 1966). This enabled the epithelium to be removed in sheets, homogenized and the subcellular components to be separated by sucrose density gradient centrifugation. In the final step a highly purified luminal membrane fraction

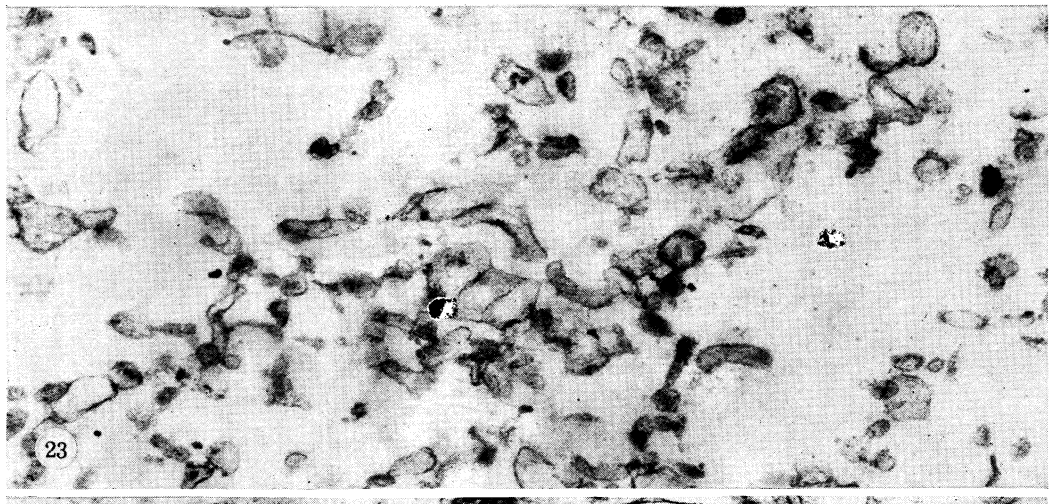

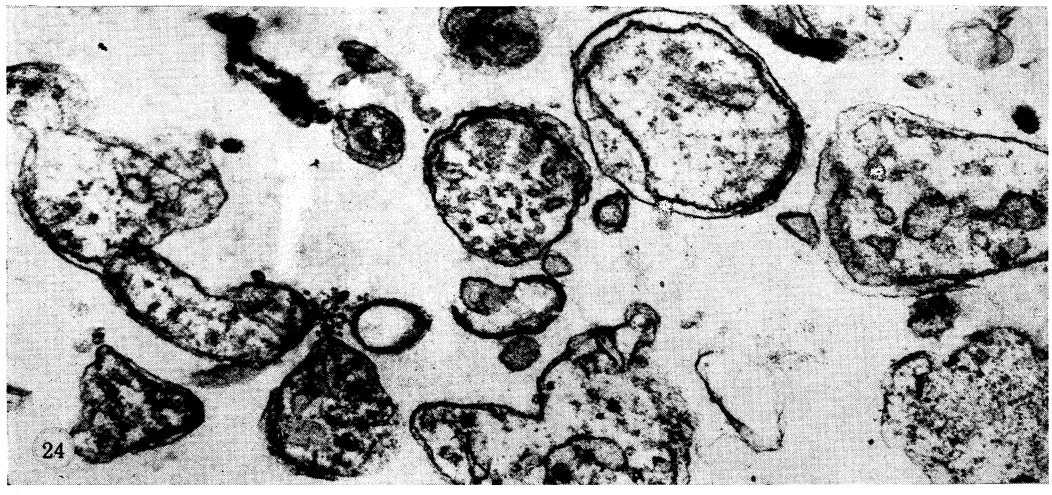

FIGURE 22. A section of pelleted bladder luminal membrane, isolated from rat bladders by the method of Hicks & Ketterer (1970). (Magn. × 50 000.)

FIGURE 23. The light membrane fraction from rat bladder, which sediments above the thick luminal membrane in the sucrose density gradient. (Magn. × 50 000.)

FIGURE 24. A part of the fraction which sediments below the luminal membrane in the density gradient. It contains mitochondria and vesicles of both thick and thin membrane. (Magn. × 50 000.)

(*Facing p.* 31)

was collected at a relative density of 1.13. The fraction above it in the gradient consisted of thin-walled vesicles and the fraction below it of larger subcellular organelles, including mitochondria. The appearance of these three fractions is shown in figures 22, 23 and 24, plate 14.

The pellet from the sucrose gradient was washed with water in order to reduce its contamination with sucrose and the yield of washed membrane from ten rats was estimated by chemical analysis to be *ca.* 200 μg.

TABLE 2. PROTEIN AND LIPIDS OF SOME PLASMA MEMBRANES

Except where otherwise indicated results in this table are taken from Korn (1969)

	protein/lipid (mass/mass)	cholesterol/ phospholipid (mol/mol)	major lipids
myelin	0.25	0.7–1.2	PC, PE, CER, CH
bladder luminal membrane†	0.7	0.6	PC, PE, CER, CH
liver cell‡	1.0–1.4	0.3–0.8	PC, PE, PS, SM, CH
Erlich ascites	2.2	—	—
intestinal microvilli	4.6	0.5–1.2	—
erythrocyte ghost	1.5–4.0	0.9–1.0	PC, PE, PS, SM, CH

PC, PE, PS, SM, CH and CER are phosphatidyl choline, phosphatidyl ethanolamine, phosphatidyl serine, sphingomyelin, cholesterol and cerebroside respectively.

† Ketterer *et al.* (1973).
‡ Dod & Gray (1968), Coleman (1968) and Touster *et al.* (1970).

(*b*) *Lipid component*

Recent views on the structure of the plasma membrane, based principally on the erythrocyte, suggest that it is a lipid protein mosaic in which the lipid component is a bi-layer with polar head groups at each surface and a hydrophobic centre. Extrinsic proteins may be attached to the surface of the membrane by electrostatic forces, but an essential characteristic of the lipid protein mosaic is the presence of intrinsic proteins having a hydrophobic region in solution in the non-polar interior of the membrane (Singer & Nicholson 1972).

In the bladder luminal plasma membrane the protein:lipid ratio (by mass) is approximately 0.7 (see table 2). Assuming conventional values for the density of lipid and protein about two thirds of the volume of the membrane is therefore lipid and the nature of this lipid presumably plays a major role in determining permeability.

In early studies in the erythrocyte, low permeability to such molecules as glycerol was associated with a high degree of saturation of the hydrocarbon. This was contributed either by the fatty acyl side chains of the phospholipids or the long-chain saturated hydrocarbon moiety of sphingomyelin (de Gier, van Deenen & van Senden 1966; O'Brien 1967). Studies of the permeability of water in artificial membrane systems have confirmed the importance of saturated hydrocarbon in restricting permeability (Finkelstein & Cass 1967; de Gier, Mandersloot & van Deenen 1968; Bittman & Blau 1972). Using liposomes, Bittman & Blau also studied the role of cholesterol in determining permeability and showed that when the lipids were in the liquid-crystal state, permeability decreased with increasing cholesterol concentration, although the reverse was true when lipids were in the crystalline state.

Chromatographic analyses of the lipids of the bladder luminal plasma membrane show four major components to be present, namely cholesterol, phosphatidyl choline, phosphatidyl

ethanolamine and cerebroside (see figure 25*a*, *b*). The presence of the sphingolipid, cerebroside, is striking.

Analysis of the fatty-acid groups released from the phospholipid component by saponification gave the surprisingly high value of 53% on a molar basis for polyunsaturated fatty acids. This may be related not to low permeability but rather to the species, since both rat erythrocyte ghost and rat liver plasma membrane are also rich in polyunsaturated fatty acids (see table 3).

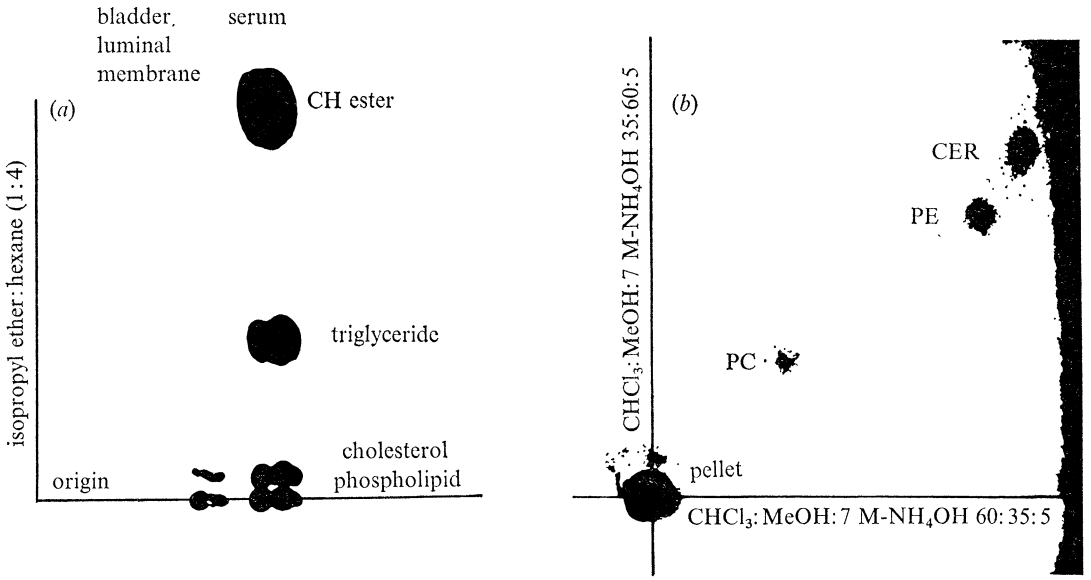

FIGURE 25. (*a*) Thin-layer chromatography of total lipids of the bladder luminal plasma membrane compared with serum lipids. The solvent was 150 propyl ether, hexane (1:4 by vol.). Spots were revealed by charring with conc. H_2SO_4.

(*b*) Two-dimensional thin-layer chromatography of the polar lipids of the bladder luminal plasma membrane. The solvent run in the first dimension was chloroform, methanol, 7 M-NH_4OH (35:60:5, by vol.). The plate was dried, reactivated *in vacuo* and run in the second dimension using the solvent mixture chloroform, methanol, 7 M-NH_4OH (60:35:5, by vol.). Spots were revealed by charring with conc. H_2SO_4. PC, PE and CER are abbreviations for phosphatidyl choline, phosphatidylethanolamine and cerebroside, respectively.

In terms of simple lipid analysis (see tables 2 and 3), the bladder luminal plasma membrane is similar to the much more permeable liver and erythrocyte plasma membranes. The one factor that is distinctive is the cerebroside content and it seems that this can have an important effect on permeability. Liposomes composed of phospholipid, cholesterol and cerebroside have been prepared by Cohen (1973) and shown to have a permeability approximately one tenth of those made of phospholipid alone (see figure 26). If the cerebroside in these liposomes were replaced by phospholipid, thereby giving rise to a membrane containing cholesterol and phospholipid in the molar ration of 1:1, the results of Bittman & Blau (1972) would lead one to expect a reduction in permeability, compared with phospholipid alone of only a third. Thus in the liposome system, cholesterol and cerebroside have similar effects in limiting permeability to water.

Clowes, Cherry & Chapman (1971) have constructed bilayers composed of phospholipid and cerebroside and find that they have an electrical resistance higher than can be attributed to the long-chain saturated hydrocarbon of the cerebroside alone. Part is attributed to the polar region. They have suggested that the galactoside head group of the cerebroside might orient both other polar head groups at the surface and also the neighbouring aqueous phase. In this respect

cerebroside behaves quite differently from sphingomyelin, which is a sphingolipid but has a phosphorylcholine polar head group.

(*c*) *The protein component*

The protein:lipid ratio of the bladder luminal plasma membrane is low compared to that of membranes other than myelin (see table 2). The unusual ultrastructure might well depend on membrane protein, more particularly intrinsic protein. It has been shown above that negative contrast staining reveals subunits which by optical processing can be seen as dodecamers of

TABLE 3. FATTY-ACID CONTENTS OF THE BLADDER LUMINAL MEMBRANE, THE ERYTHROCYTE GHOST AND THE LIVER PLASMA MEMBRANE OF THE RAT

fatty acid		bladder luminal membrane† mol %	erythrocyte ghost‡ mol %	liver plasma membrane§ mol %
palmitic acid	(16:0)	12.2	44	22.9
stearic acid	(18:0)	16.6	22	29.8
oleic acid	(18:1)	18.7	18	10.2
linoleic acid	(18:2)	24.9	14	13.1
linolenic acid	(18:3)	3.5	—	—
licosatrienoic acid	(20:3)	5.9	—	0.9
arachidonic acid	(20:4)	18.2	17	16.7
others	—	—	—	6.4

† Ketterer *et al.* (1973). ‡ Maddy (1966). § Wood (1970).

particles 3 nm in diameter. Similar images have been observed in negative-contrast-stained preparations of the frog retinal disk and shown to be the protein rhodopsin (Blasie, Worthington & Dewey 1969; Blasie & Worthington 1969). As pointed out earlier, when the bladder luminal plasma membrane is subjected to freeze-etching the components of the subunits are seen, not

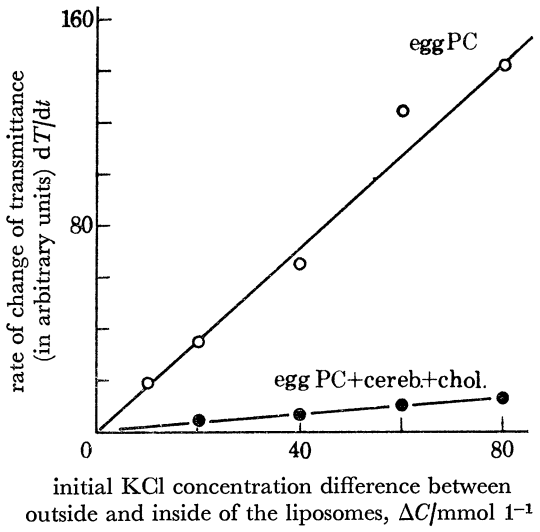

FIGURE 26. Effect of lipid composition of liposomes on their permeability to water. The slopes of the curves are proportional to the water permeability. ○, Egg phosphatidyl choline and dipalmitoyl phosphatidic acid, (96:4); ●, egg phosphatidyl choline cerebrosides, cholesterol and dipalmitoyl phosphatidic acid (24:24:48:4). (Ratios in parenthesis are molar.)

as particles, but as rods passing through the membrane (Staehelin *et al.* 1972). Similar structures have been seen in freeze-etched erythrocytes and shown to be the glycoprotein now known as glycophorin (Pinto da Silva, Douglas & Branton 1971; Segrest, Kahane, Jackson & Marchesi 1973). One can therefore envisage that the bladder luminal membrane might consist of monomeric protein rods 3 nm in diameter and 12 nm in length. Such proteins would have a molecular mass of 70000. It can be calculated that they would occupy about 23% of the plaque area and therefore account for approximately 50% of the membrane protein, depending on how it is distributed between plaque and hinge areas. However, when an attempt was made to disperse the membrane proteins and separate them according to molecular mass, the component of molecular mass 70000 was not predominant (see figure 27*a*). The analysis of proteins was complex whether the separation was made by molecular mass or isoelectric point (see figure 27*b*).

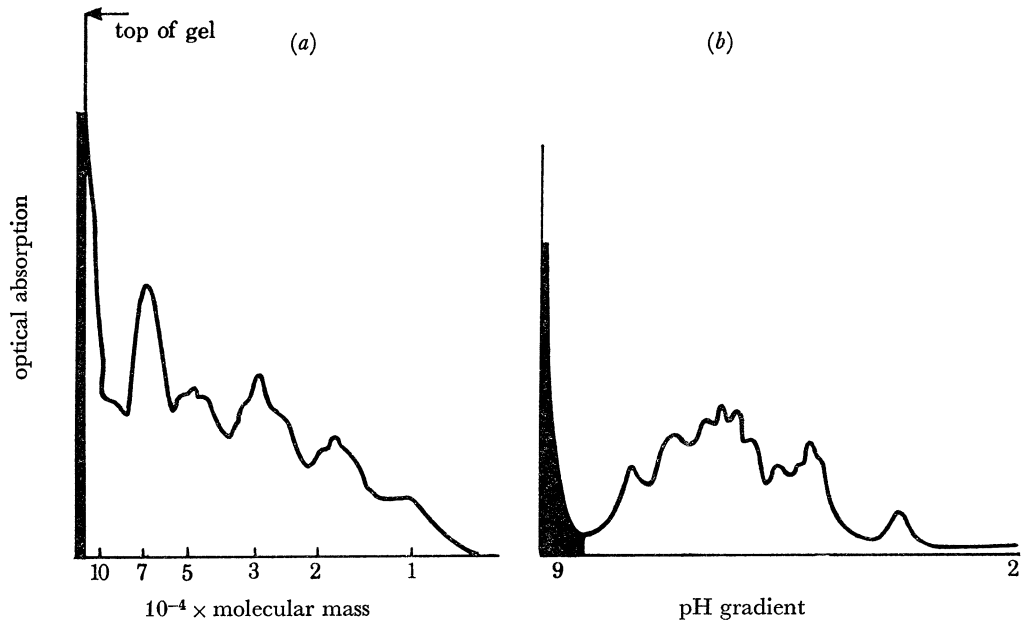

FIGURE 27. (*a*) Gel electrophoresis in sodium dodecyl sulphate, urea of the proteins of the bladder luminal plasma membrane. Gels were 7% acrylamide, 8 M urea and 1% (mass/vol.) sodium dodecyl sulphate. Protein was stained with naphthalene black and carbohydrate with the Feulgen periodic acid–Schiff reagent. Mucoprotein is shown black on graphs.

(*b*) Gel isoelectric focusing in Triton X-100, urea of proteins of the bladder luminal plasma membrane. Gels were 5% polyacrylamide, with 0.3% of 40% (mass/vol.) Ampholine pH 3 to 10. Protein was stained with Coomassie blue and carbohydrate with Fuelgen periodic acid-Schiff reagent.

It should be noted that some protein, including all mucoprotein, remains undispersed. The patterns which were obtained only from those proteins which did disperse may therefore be misleading. The large particle mass mucoprotein may play an important part in the subunit structure. This possibility is supported by the observation above, that sodium dodecyl sulphate, which is used to disperse the membrane proteins for electrophoresis, when added to the bladder luminal membrane *in situ*, seems to cause the whole subunits to be detached without breakdown of the subunits themselves.

(*d*) *Amino acid analysis*

So far the bladder luminal plasma membrane has two markers, an unusual morphology and a high cerebroside content. Its amino acid analysis reveals another marker, namely the high

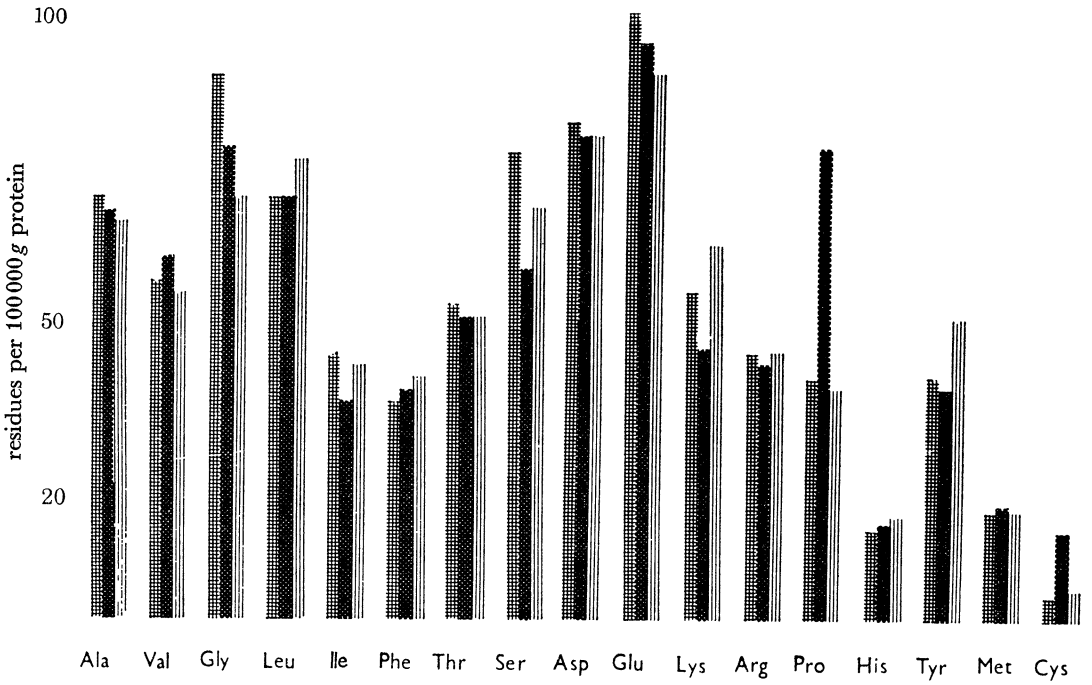

FIGURE 28. A comparison of the amino acid analysis of the bladder luminal plasma membrane fraction with the analyses of the fractions above and below it in the sucrose density gradient (see figures 22 to 24).

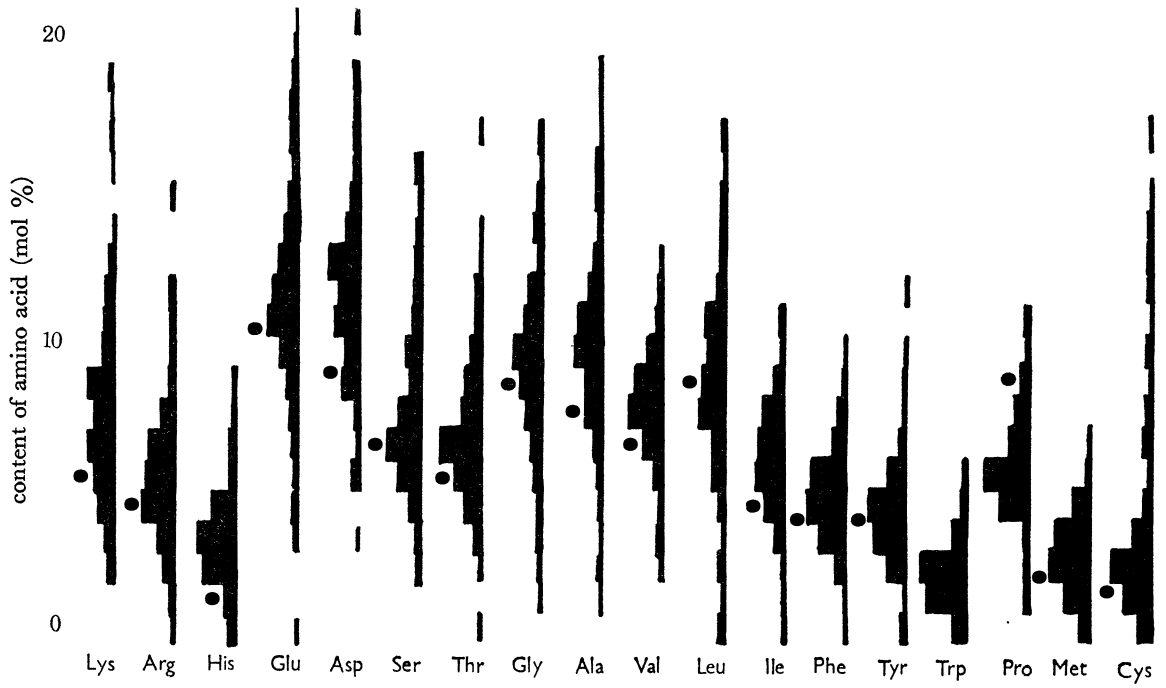

FIGURE 29. A comparison of the amino acid analysis of the bladder luminal plasma membrane with that of some 200 pure proteins (Reeck 1970). The frequency of content of each amino acid in the pure proteins is represented in a separate histogram. In each histogram the ordinate represents the content of each amino acid in moles %, simplified so that values falling in between two whole numbers are considered together. Thus the first category is 0 mol %, the second 0 to 1 mol %, the third 1 to 2 mol % and so on. The abscissa represents the number of proteins from 0 to 100 in which each content is found. The analysis of the bladder luminal plasma membrane is shown as spots superimposed upon the histograms.

proline content of 8.4 mol %. This distinguishes it clearly from the fractions above and below it in the sucrose density gradient in which it separates (see figure 28).

When compared with amino acid analyses of some 200 purified proteins it is seen to be unusually proline-rich (see figure 29).

Proline residues are unique among amino acid residues in providing no peptide bond hydrogen bond donor. As a result they are capable of having important effects on protein conformation. It has been observed that 8 mol % of randomly distributed proline residues can deform the polypeptide into a random coil. High concentrations of proline residues within a sequence can cause the formation of structures with the properties of polyproline, a structure with unusual characteristics (Szent-Gyorgy & Cohen 1957). Polyproline has repeating peptide carbonyl groups which make it essentially hydrophilic. However, it is capable of undergoing *cis–trans* mutarotation and consequent conformation changes according to the solvent environment (Carver & Blout 1967).

Proline may have a specific role to play in membrane structure and function. For example, rhodopsin has 7 mol % and, even more intriguing, glycophorin has a C-terminal peptide which is 16 mol % proline. This part of the molecule is believed to be at the intracellular surface (Segrest *et al.* 1973).

6. Conclusions

How does the chemical knowledge we have obtained relate to structure and function?

(*a*) *Structure*

In section, the bladder luminal plasma membrane is characterized by a thick densely staining outer leaflet. This may be related to the large particle mass mucoprotein compound, the carbohydrate moiety of which, in line with other plasma membranes (Singer & Nicholson 1972), should be on the outer surface. Certainly, the outer surface has a high affinity for colloidal iron (see figure 30). No correlation has been made as yet between any protein component and subunit structure. The present interpretation would be that subunit structure is the result of complex interactions.

(*b*) *Barrier function*

With regard to permeability, there seems little doubt that cerebroside has an important effect in lowering water permeability. Cholesterol assists in maintaining a condensed lipid layer. Even so, the proper function of the lipid layer must depend on its being maintained in a condensed state during the mechanical stress of bladder contraction. This may be the reason for the rigidity of the plaque regions. The substructure may control rigidity and thereby the denseness of packing of the lipid phase.

One other contribution to barrier function which has not been touched on as yet because so little is known of it, is the possible presence of ordered water. The carbohydrate moieties of glycoprotein and glycolipid and the carbonyl moieties of proline if suitably oriented could order water in such a way that permeability is considerably reduced.

Some of the questions raised could be answered if more membrane were available for study. To this end, slaughter-house material is being examined as a possible source.

R. M. Hicks and B. Ketterer are supported by generous grants from the Cancer Research Campaign and R. C. Warren is in receipt of a Junior Research Fellowship from the Medical Research Council. We wish to thank our technicians, Mr A. L. Barron, Miss L. Christodoulides,

Miss C. Page and Mr J. Wilkes, for their assistance, and Dr A. Bangham, Dr D. Beale, Dr J. A. Firth, Professor R. W. Horne, Dr G. L. Mills, Miss H. Sanders, Mr C. D. Stubbs, Professor J. F. Tait and Mr J. St J. Wakefield for their help and interest in the work.

REFERENCES (Hicks *et al.*)

Bittman, R. & Blau, L. 1972 The phospholipid–cholesterol interaction. Kinetics of water permeability in liposomes. *Biochemistry* **11**, 4831–4838.

Blandy, J. P. 1964 The feasibility of preparing an ideal substitute for the urinary bladder. *A. R. Coll. Surg. Eng.* **35**, 287–311.

Blasie, J. K. & Worthington, C. R. 1969 Planar liquid-like arrangement of photopigment molecules in frog retinal receptor disc membranes. *J. molec. Biol.* **39**, 417–439.

Blasie, J. K., Worthington, C. R. & Dewey, M. M. 1969 Molecular localization of frog retinal receptor photopigment by electron microscopy and low angle X-ray diffraction. *J. molec. Biol.* **39**, 407–416.

Carver, J. P. & Blout, E. R. 1967 Polypeptide models for collagen. In *Treatise on collagen.* Vol. 1. *Chemistry of collagen* (ed. Ramachandran, G. N.), pp. 441–526. New York: Academic Press.

Chlapowski, F. J., Bonneville, M. A. & Staehelin, L. A. 1972 Lumenal plasma membrane of the urinary bladder. II. Isolation and structure of membrane components. *J. Cell Biol.* **53**, 92–104.

Clowes, A. W., Cherry, R. J. & Chapman, D. 1971 Physical properties of lecithin-cerebroside bilayers. *Biochim. biophys. Acta* **249**, 301–317.

Cohen, E. 1973 A study of the permeability of small non electrolytes through model membranes. Ph.D. Dissertation, University of Cambridge.

Coleman, R. 1968 Some features of the lipid composition of rat liver surface and cytoplasmic membranes. *Chem. Phys. Lipids* **2**, 144–146.

Dod, B. J. & Gray, G. M. 1968 The lipid composition of rat-liver plasma membranes. *Biochim. biophys. Acta* **150**, 397–404.

Englund, S. E. 1956 Observations on the migration of some labelled substances between the urinary bladder and blood in rabbit. *Acta Radiol. Suppl.* **135**, 9–78.

Finkelstein, A. & Cass, A. 1967 Effect of cholesterol on water permeability of lipid membranes. *Nature, Lond.* **216**, 717–718.

Firth, J. A. & Hicks, R. M. 1971 Ultrastructural and cytochemical features of transitional epithelium in mammals. *J. Anat., Lond.* **110**, 151-152.

Firth, J. A. & Hicks, R. M. 1973 Interspecies variation in the fine structure and enzyme cytochemistry of mammalian transitional epithelium. *J. Anat., Lond.* **116**, 31–43

Fraser, R. D. B. & Millward, G. R. 1970 Image averaging by optical filtering. *J. ultrastruct. Res.* **31**, 203–211.

de Gier, J., van Deenen, L. L. M. & van Senden, K. G. 1966 Glycerol permeability of erythrocytes. *Experientia* **22**, 20–21.

de Gier, J., Mandersloot, J. G. & van Deenen, L. L. M. 1968 Lipid composition and permeability of liposomes. *Biochim. biophys. Acta* **150**, 666–675.

Hicks, R. M. 1965 The fine structure of the transitional epithelium of rat ureter. *J. Cell Biol.* **26**, 25–48.

Hicks, R. M. 1966*a* The permeability of rat transitional epithelium. *J. Cell Biol.* **28**, 21–31.

Hicks, R. M. 1966*b* The function of the Golgi complex in transitional epithelium. *J. Cell Biol.* **30**, 623–644.

Hicks, R. M. & Ketterer, B. 1969 Hexagonal lattice of subunits in the thick luminal membrane of the rat urinary bladder. *Nature, Lond.* **224**, 1034–1035.

Hicks, R. M. & Ketterer, B. 1970 Isolation of the plasma membrane of the luminal surface of rat bladder epithelium, and the occurrence of a hexagonal lattice of subunits both in negatively stained whole mounts and in sectioned membranes. *J. Cell Biol.* **45**, 542–553.

Johnson, J. A., Cavert, H. M., Lifson, N. & Visscher, M. B. 1951 Permeability of the bladder to water studied by means of isotopes. *Am. J. Physiol.* **165**, 87–92.

Kerr, W. K., Barkin, M., D'Aloisio, J. & Menczyk, Z. 1963 Observations on the movement of ions and water across the wall of the human bladder and ureter. *J. Urol.* **89**, 812–819.

Ketterer, B., Hicks, R. M., Christodoulides, L. & Beale, D. 1973 Studies of the chemistry of the luminal plasma membrane of rat bladder epithelial cells. *Biochim. biophys. Acta* **311**, 180–190.

Klug, A. & De Rosier, D. J. 1966 Optical filtering of electron micrographs: reconstruction of one-sided images. *Nature, Lond.* **212**, 29–32.

Korn, E. D. 1969 Cell membranes: structure and synthesis. *Ann. Rev. Biochem.* **38**, 263–288.

Koss, L. G. 1969 The asymmetric unit membranes of the epithelium of the urinary bladder of the rat. An electron microscopic study of a mechanism of epithelial maturation and function. *Lab. Invest.* **21**, 154–168.

Levinsky, N. G. & Berliner, R. W. 1959 Changes in composition of the urine in ureter and bladder at low urine flow. *Am. J. Physiol.* **196**, 549–553.

Maddy, A. H. 1966 The chemical organization of the plasma membrane of animal cells. *Int. Rev. Cytol.* **20**, 1–65.

Markham, R., Hitchborn, J. H., Hills, G. J. & Frey, S. 1964 The anatomy of tobacco mosaic virus. *Virology*, **22** 342–359.

Marucci, H. D., Shoemaker, W. C., Wase, A. W., Strauss, H. D. & Geyer, S. V. 1954 Permeability of normal and artificially constructed canine urinary bladders to I^{131}, Na^{22} and P^{32}. *Proc. Soc. exp. Biol. Med.* **87**, 569–571.

McIntyre, K. H. & Williams, V. J. 1969 The role of the bladder in nitrogen retention in sheep. *Aust. J. exp. Biol. med. Sci.* **47**, 633–635.

O'Brien, J. S. 1967 Cell membranes. Composition: structure: function. *J. theoret. Biol.* **15**, 307–324.

Pinto da Silva, P., Douglas, S. D. & Branton, D. 1971 Localization of A antigen sites on human erythrocyte ghosts. *Nature, Lond.* **232**, 194–196.

Porter, K. R., Kenyon, K. & Badenhausen, S. 1967 Specialization of the unit membrane. *Protoplasma* **63**, 262–274.

Rapoport, A., Nicholson, T. F. & Yendt, E. R. 1960 Movement of electrolytes across the wall of the urinary bladder in dogs. *Am. J. Physiol.* **198**, 191–194.

Reeck, G. 1970 In *Handbook of biochemistry* (ed. H. A. Sober), pp. c 281–287. Cleveland: Chemical Rubber Company.

Segrest, J. P., Kahane, I., Jackson, R. L. & Marchesi, V. T. 1973 Major glycoprotein of the human erythrocyte. Evidence for an amphipathic molecular structure. *Archs Biochem. Biophys.* **155**, 167–183.

Singer, S. J. & Nicholson, G. L. 1972 The fluid mosaic model of the structure of cell membranes. *Science, N.Y.* **175**, 720–731.

Staehelin, L. A., Chlapowski, F. J. & Bonneville, M. A. 1972 Lumenal plasma membrane of the urinary bladder. 1. Three-dimensional reconstruction from freeze-etch images. *J. Cell Biol.* **53**, 73–91.

Szent-Gyorgyi, A. G. & Cohen, C. 1957 Role of proline in polypeptide chain configuration of proteins. *Science, N.Y.* **126**, 697–698.

Touster, O., Aronson, N. N., Dulaney, J. T. & Hendrickson, H. 1970 Isolation of rat plasma membranes. Use of nucleotide pyrophosphatase and phosphodiesterase 1 as marker enzymes. *J. Cell Biol.* **47**, 604–618.

Vergara, J., Longley, W. & Robertson, J. D. 1969 A hexagonal arrangement of subunits in membrane of mouse urinary bladder. *J. molec. Biol.* **46**, 593–596.

Warren, R. L. 1959 A versatile micro-sample flame spectrophotometer. *Colloquium Spectroscopicum Internationale*, vol. 8, pp. 213–215. Aarau, Switzerland: Verlag, Sauerlander & Co.

Warren, L., Glick, M. C. & Nass, M. K. 1966 Membranes of animal cells. I. Methods of isolation of the surface membrane. *J. Cell Physiol.* **68**, 269–287.

Warren, R. C. & Hicks, R. M. 1970 Structure of the subunits in the thick luminal membrane of rat urinary bladder. *Nature, Lond.* **227**, 280–281.

Warren, R. C. & Hicks, R. M. 1971 A simple method of linear integration for resolving structure in periodic lattices: application to an animal cell membrane and a crystalline inclusion. *J. ultrastruct. Res.* **36**, 861–874.

Wood, R. 1970 Plasma membranes: structural analyses of neutral lipids and phospholipids of rat liver. *Archs Biochem. Biophys.* **141**, 174–182.

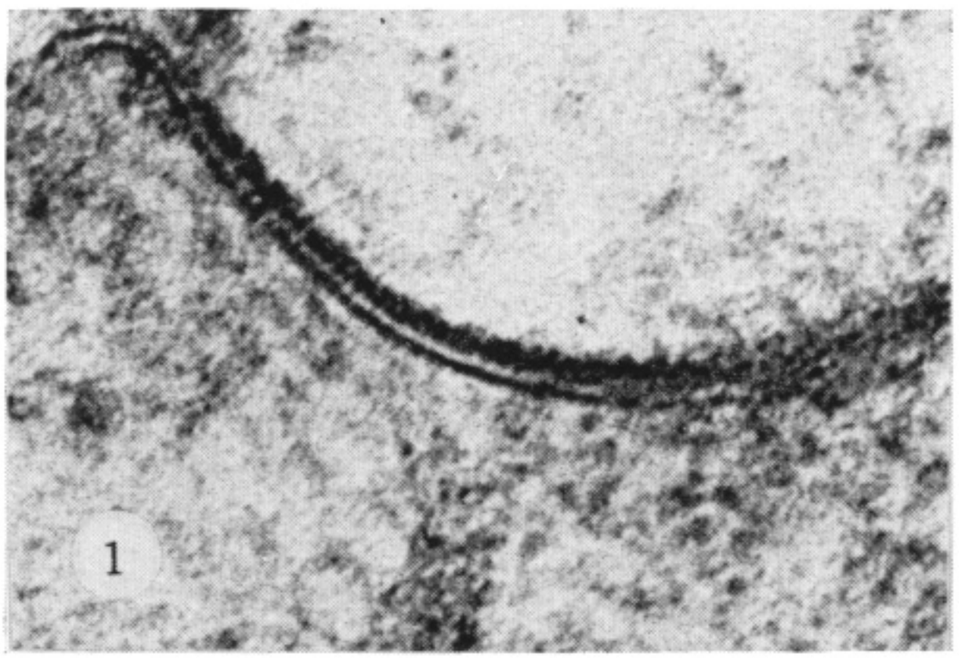

FIGURE 1. Cross-section of a portion of the cell membrane limiting a rat bladder epithelium superficial cell. Where the membrane is sharply bent it is about 8 nm thick and the two densely staining laminae are of about the same thickness. In the plaque region it is about 12 nm across, and the outer dense lamina adjacent to the urine is markedly thicker than that adjacent to the cytoplasm. Substructure is visible in the outer lamina. The tissue was fixed in phosphate-buffered osmium tetroxide and embedded in Epon and the thin section was contrast-stained with lead and uranyl salts. (Magn. × 200 000.)

FIGURE 2. Section of luminal cell cytoplasm in the rat bladder epithelium. The surface of the cell is limited by a rigid, angular membrane, with an easily resolved, trilaminate structure. This membrane also forms fusiform vacuoles in the cytoplasm. Tissue prepared as for figure 1. (Magn. × 60 000.)

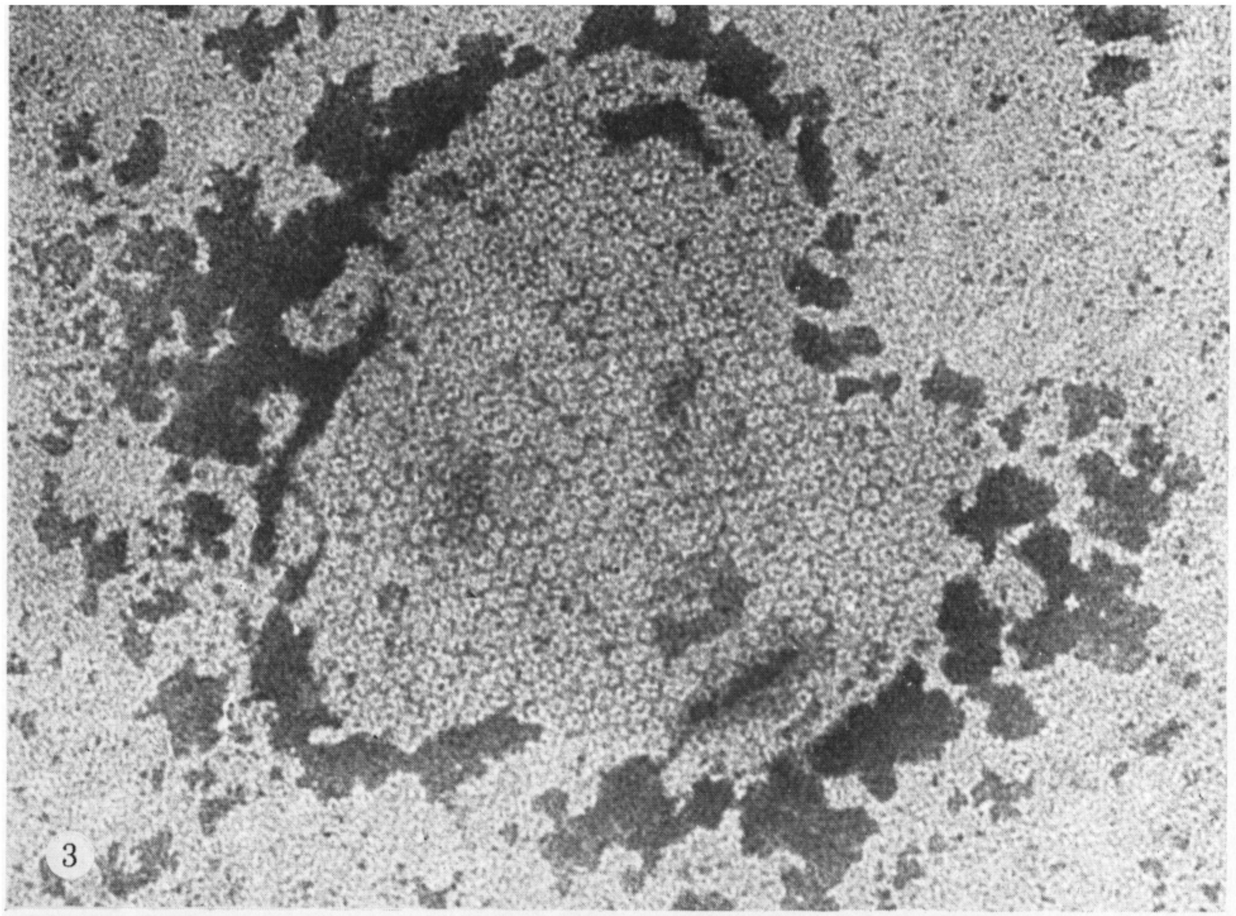

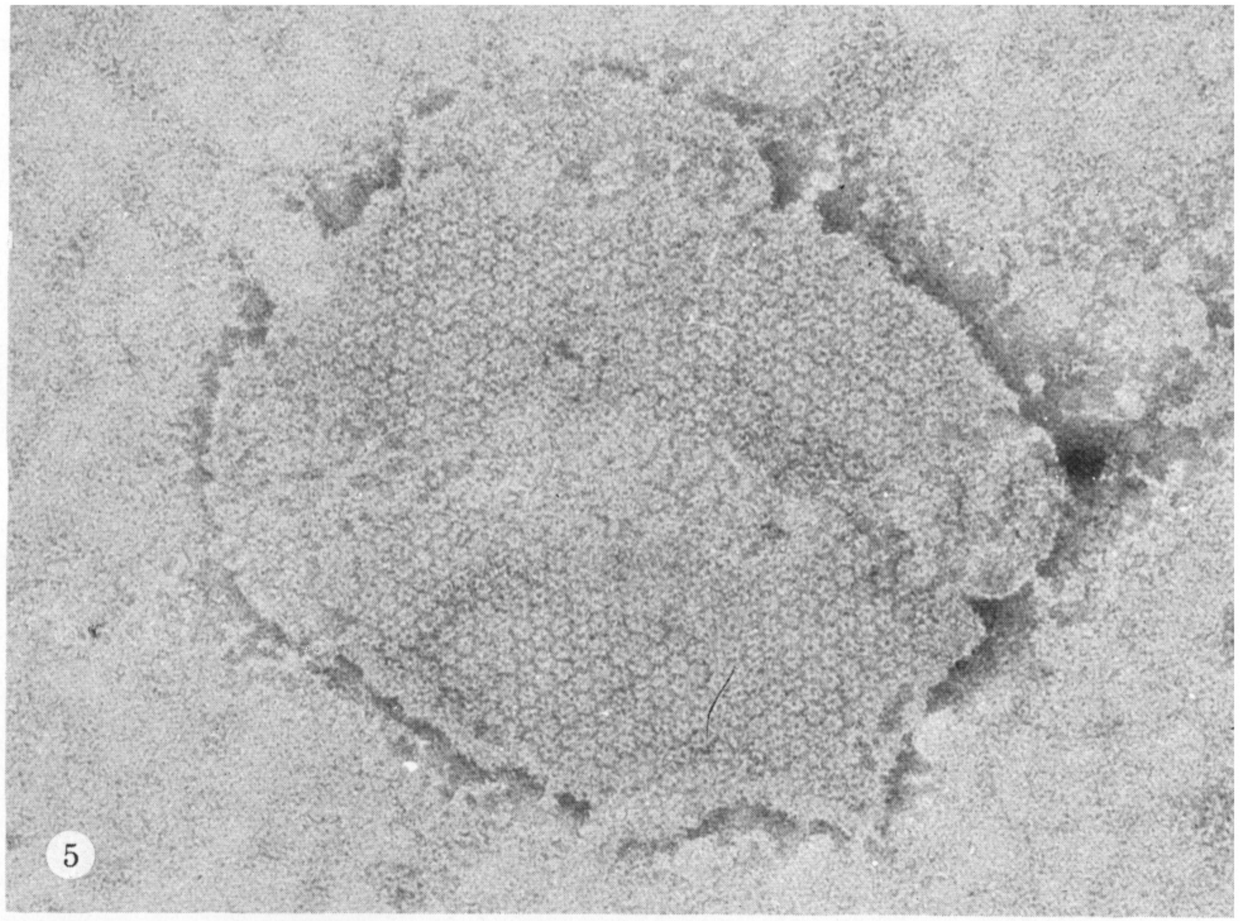

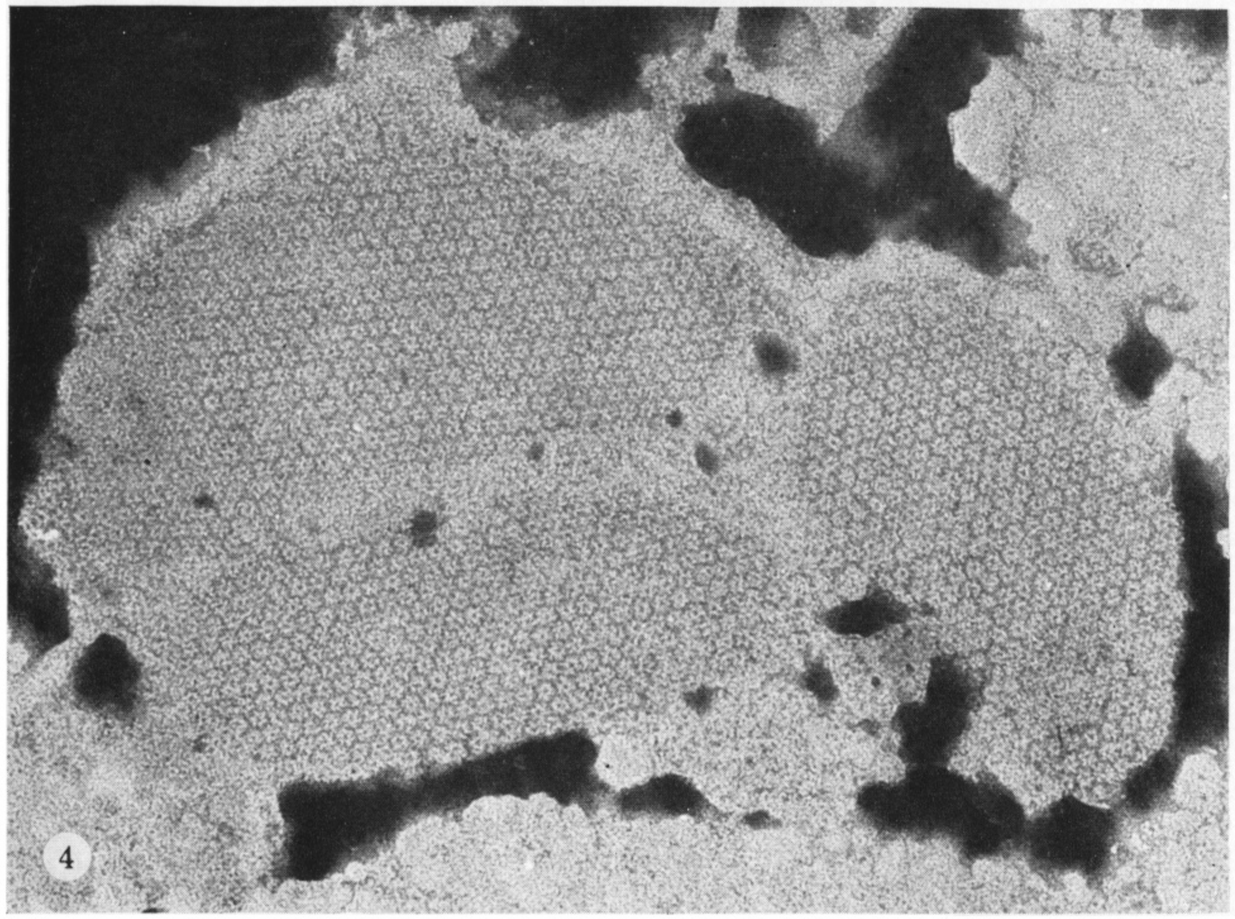

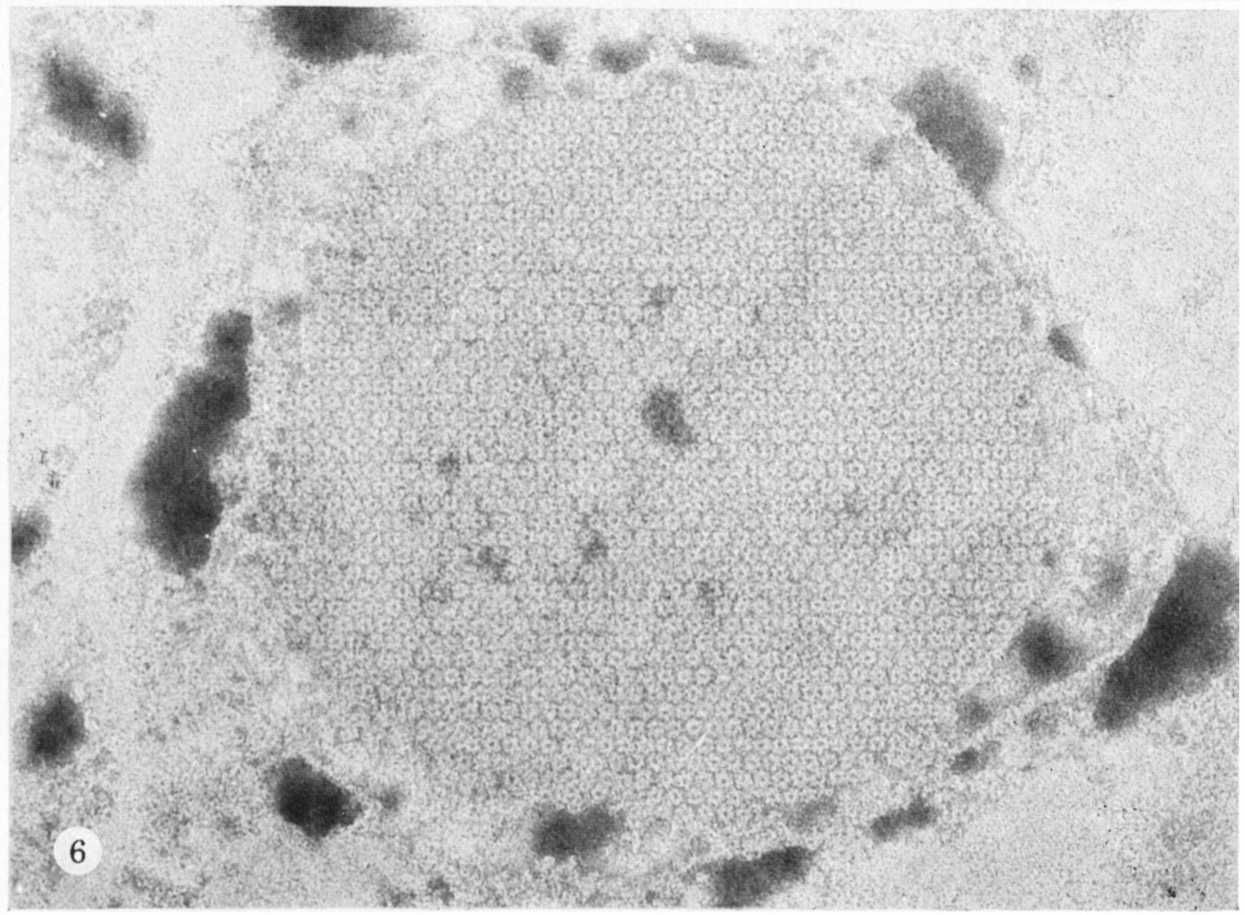

FIGURES 3 to 6. For description see opposite

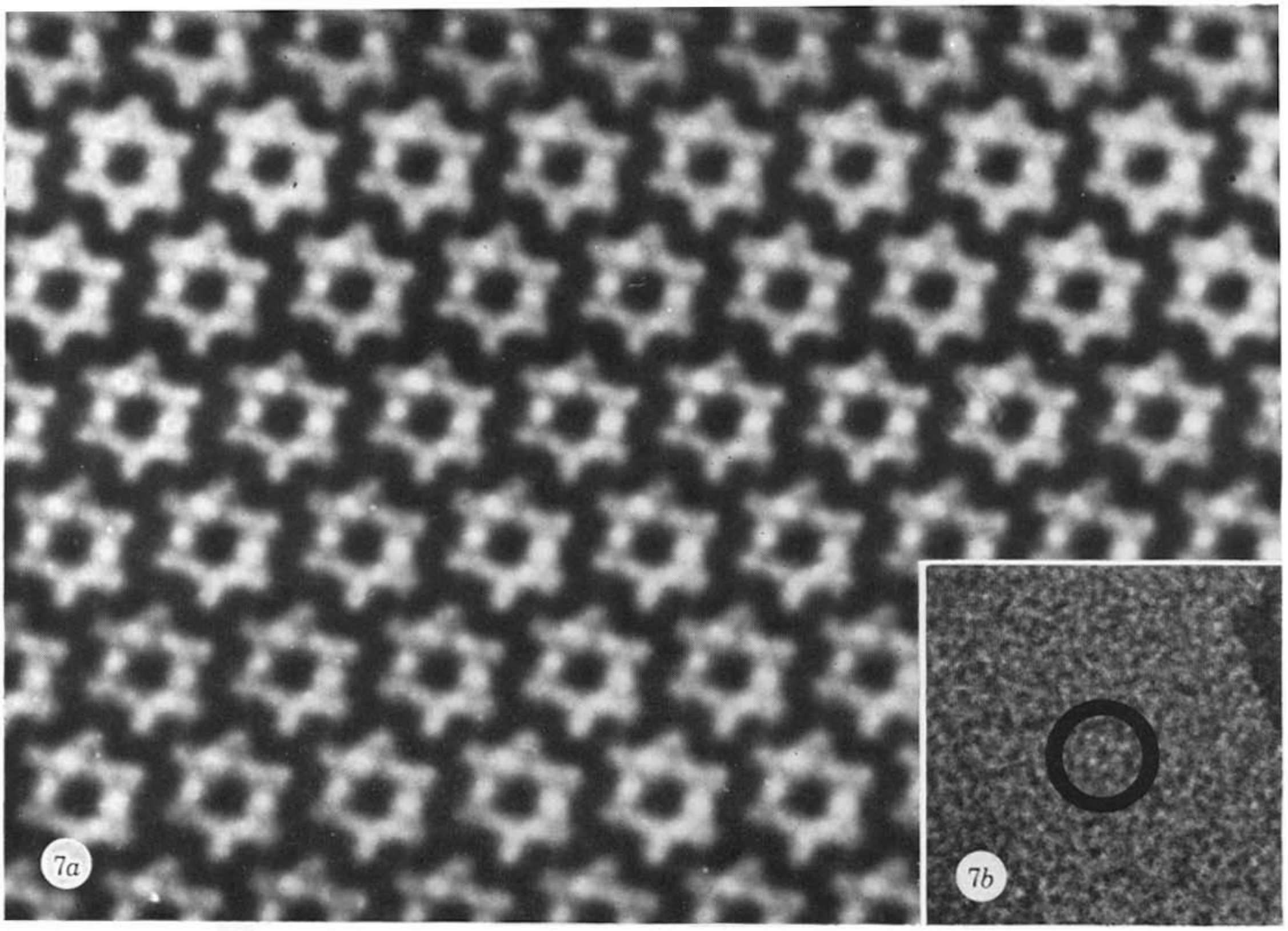

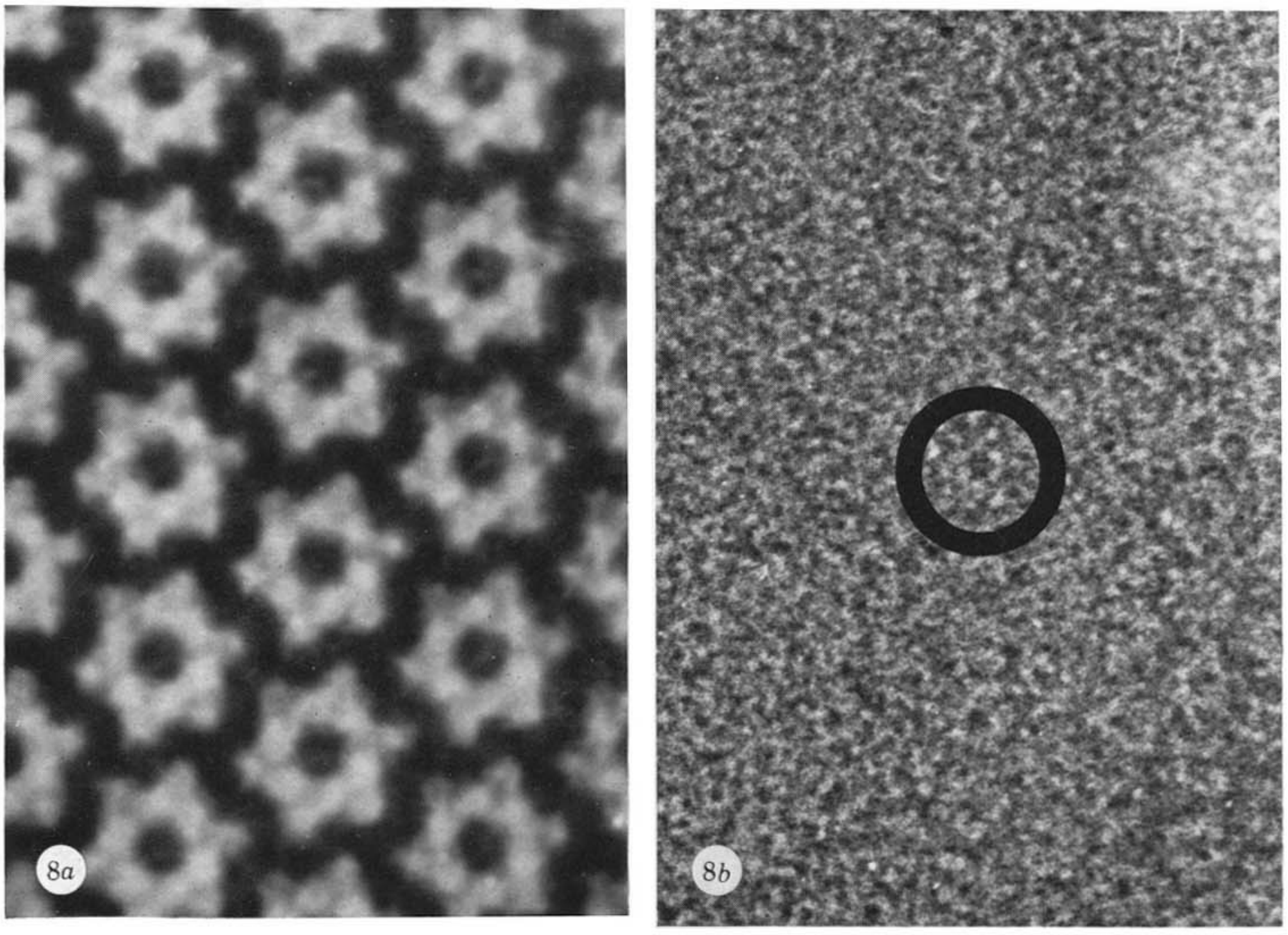

FIGURE 7. (*a*) Negatively stained rat bladder luminal membrane, processed by linear integration. Each subunit is composed of 12 particles of diameter 3 nm, and is skewed by 19° to the axis of the lattice. (Magn. × 1 100 000.) (*b*) Unprocessed image showing central particles. (Magn. × 440 000.)

FIGURE 8. (*a*) Integrated image showing central particles (Magn. × 1 600 000). (*b*) Unprocessed image showing central particle (Magn. × 680 000).

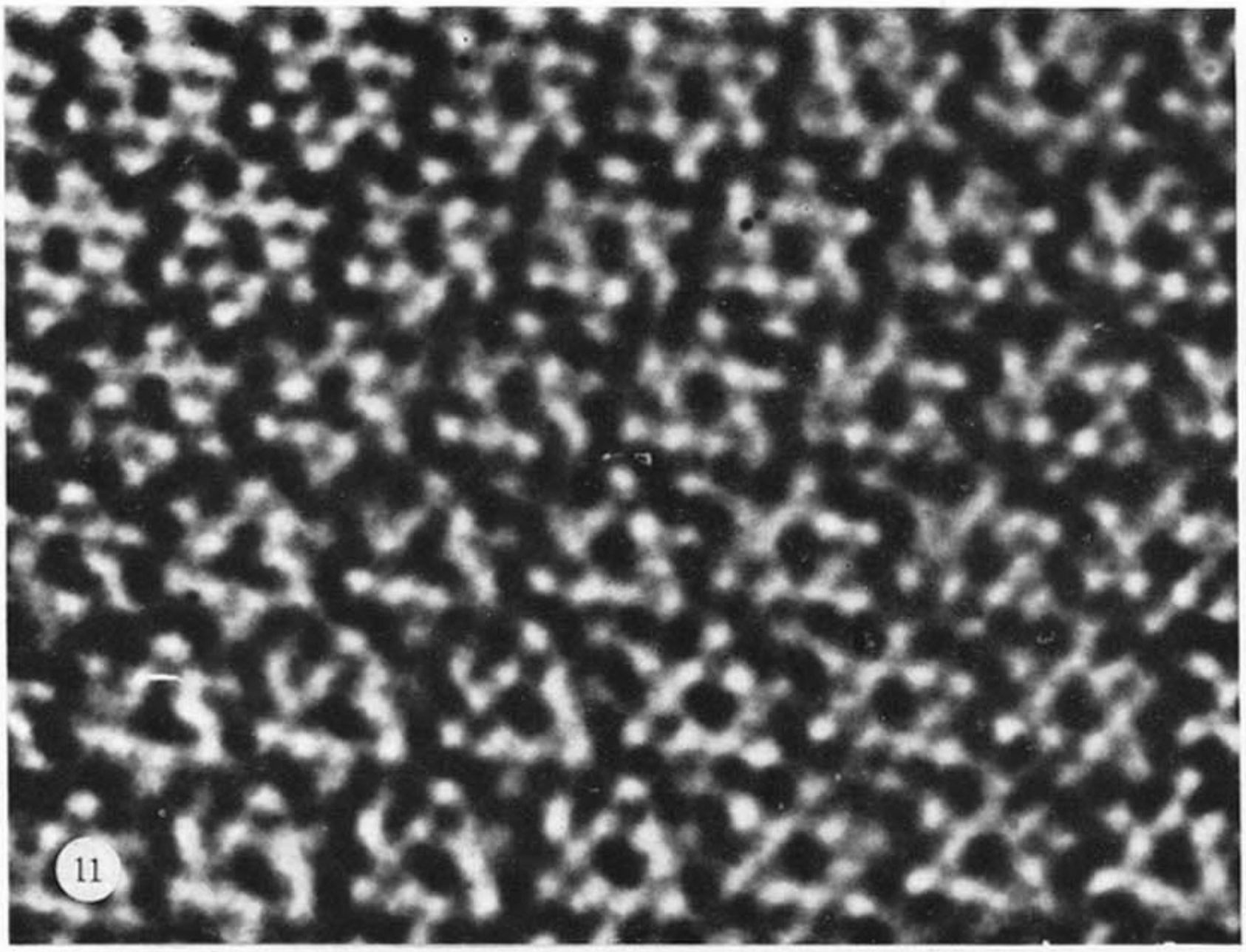

11

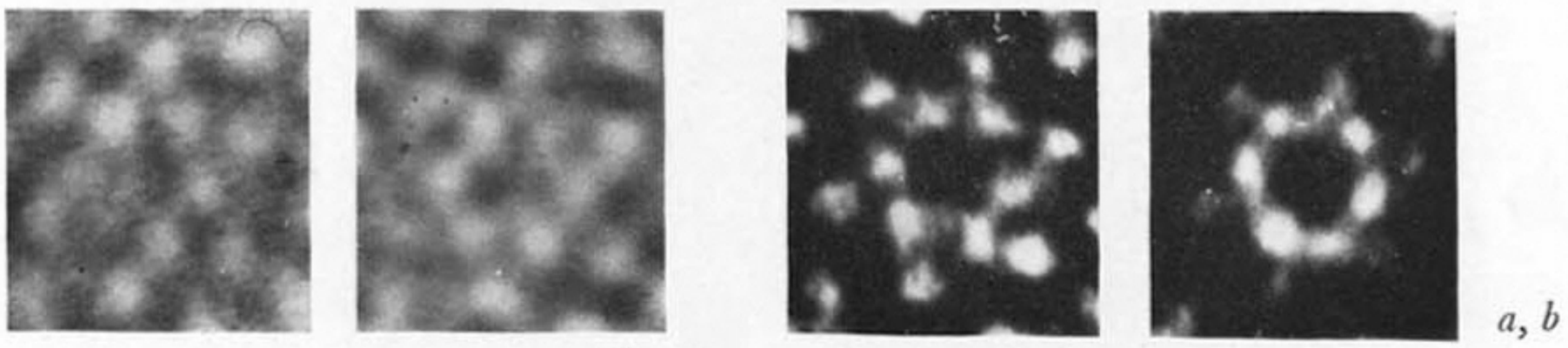

a, b

a, b

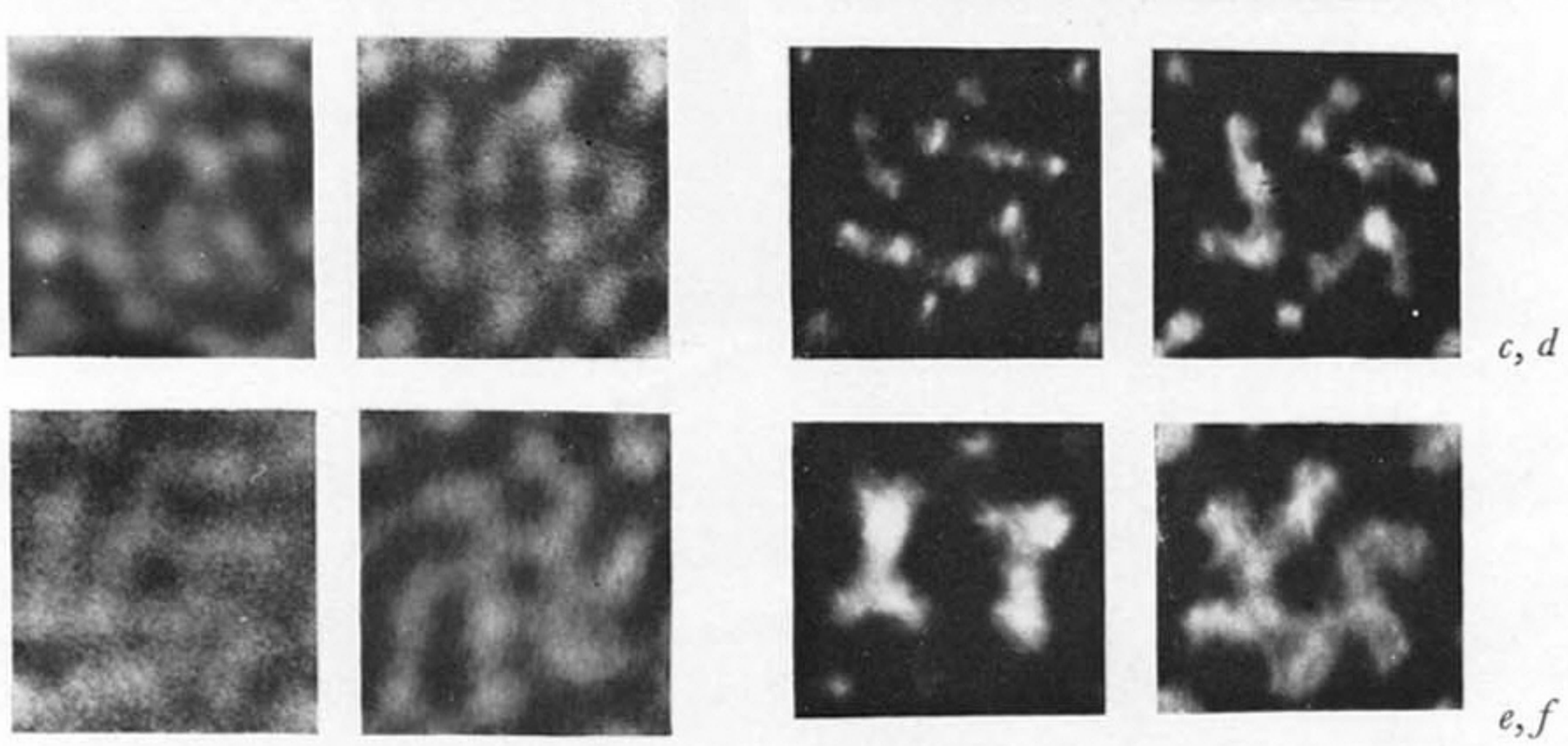

c, d

c, d

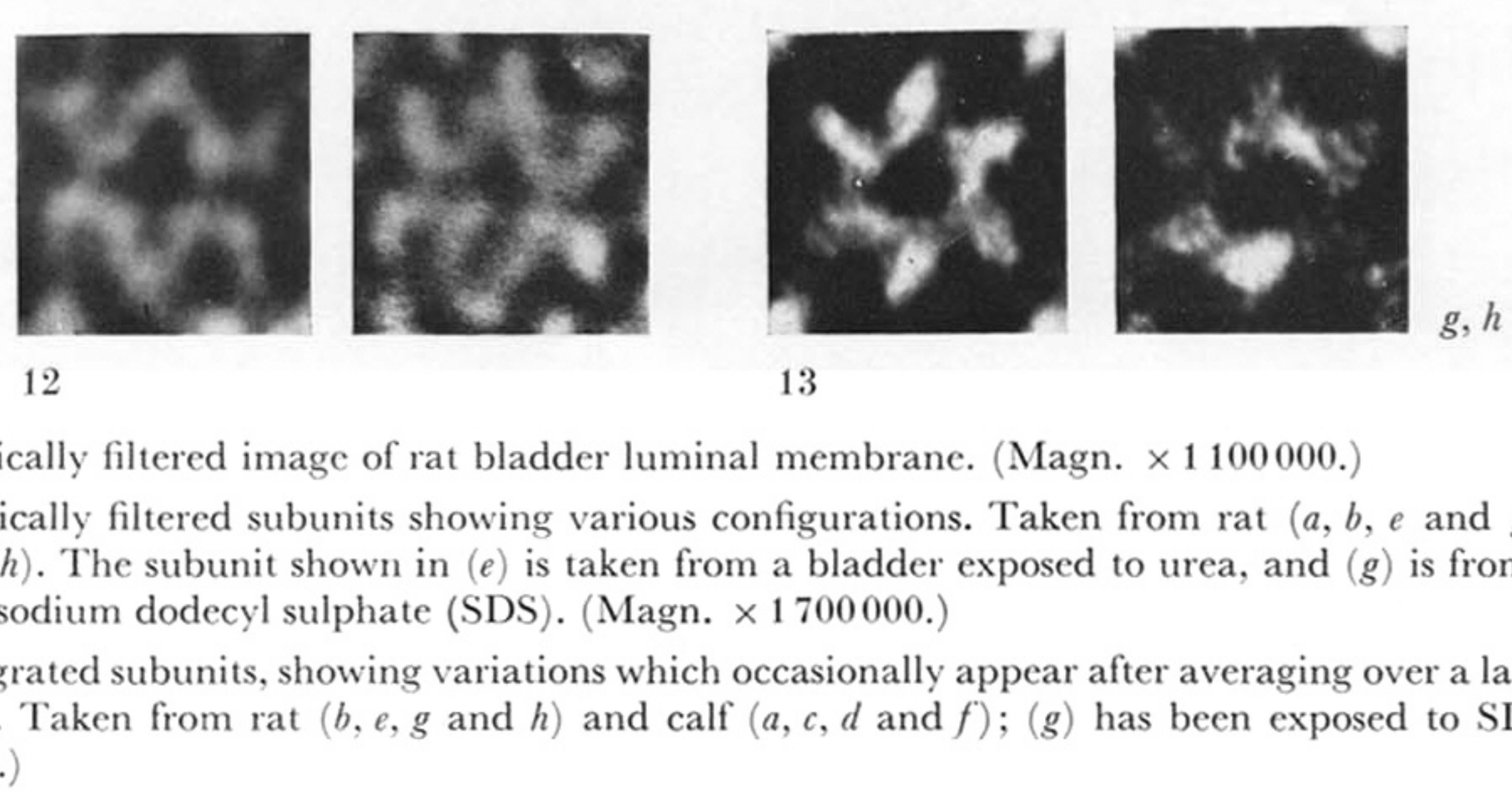

e, f

e, f

g, h

g, h

12

13

FIGURE 11. Optically filtered image of rat bladder luminal membrane. (Magn. × 1 100 000.)

FIGURE 12. Optically filtered subunits showing various configurations. Taken from rat (*a*, *b*, *e* and *g*) and calf (*c*, *d*, *f* and *h*). The subunit shown in (*e*) is taken from a bladder exposed to urea, and (*g*) is from a bladder exposed to sodium dodecyl sulphate (SDS). (Magn. × 1 700 000.)

FIGURE 13. Integrated subunits, showing variations which occasionally appear after averaging over a large number of subunits. Taken from rat (*b*, *e*, *g* and *h*) and calf (*a*, *c*, *d* and *f*); (*g*) has been exposed to SDS. (Magn. × 1 700 000.)

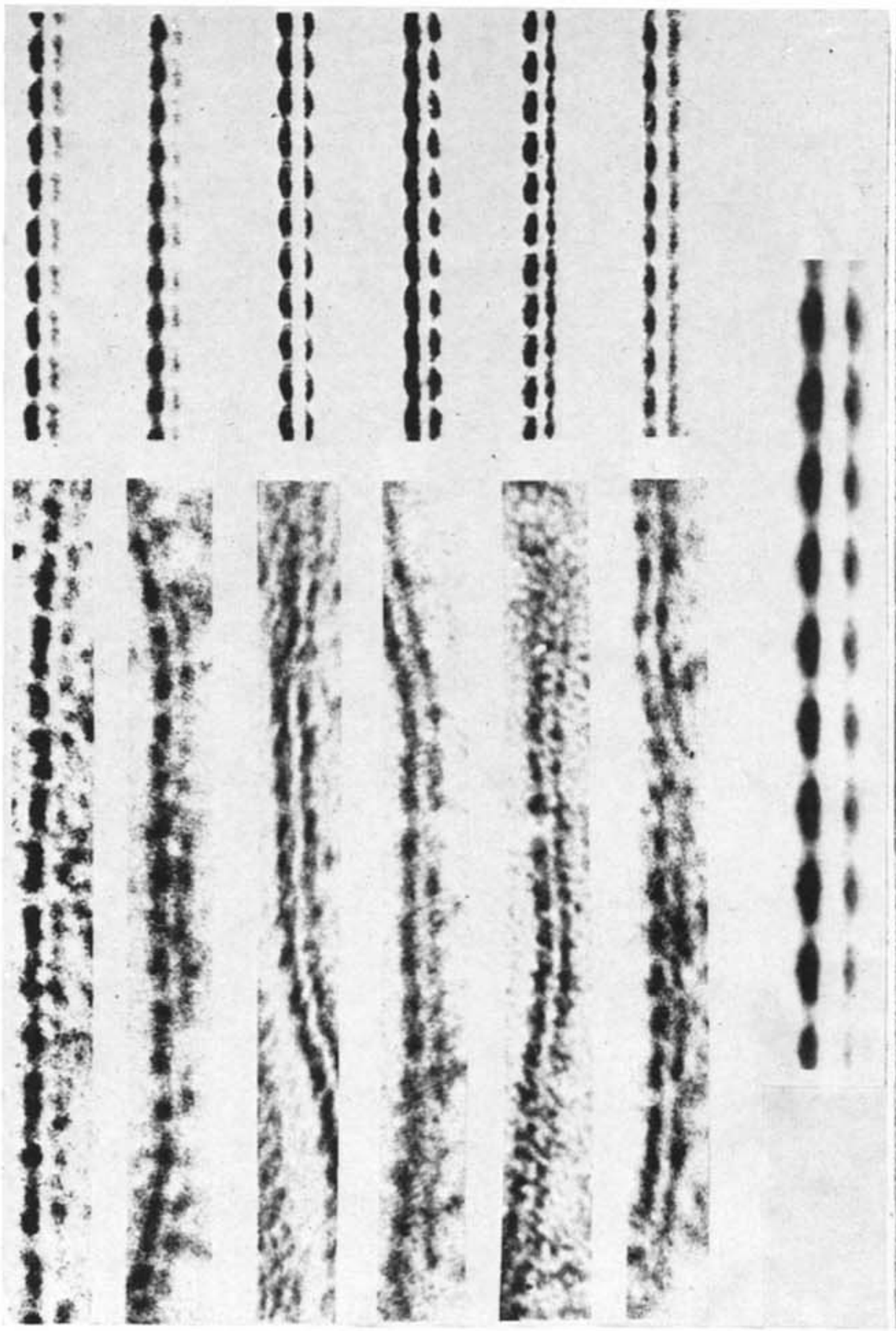

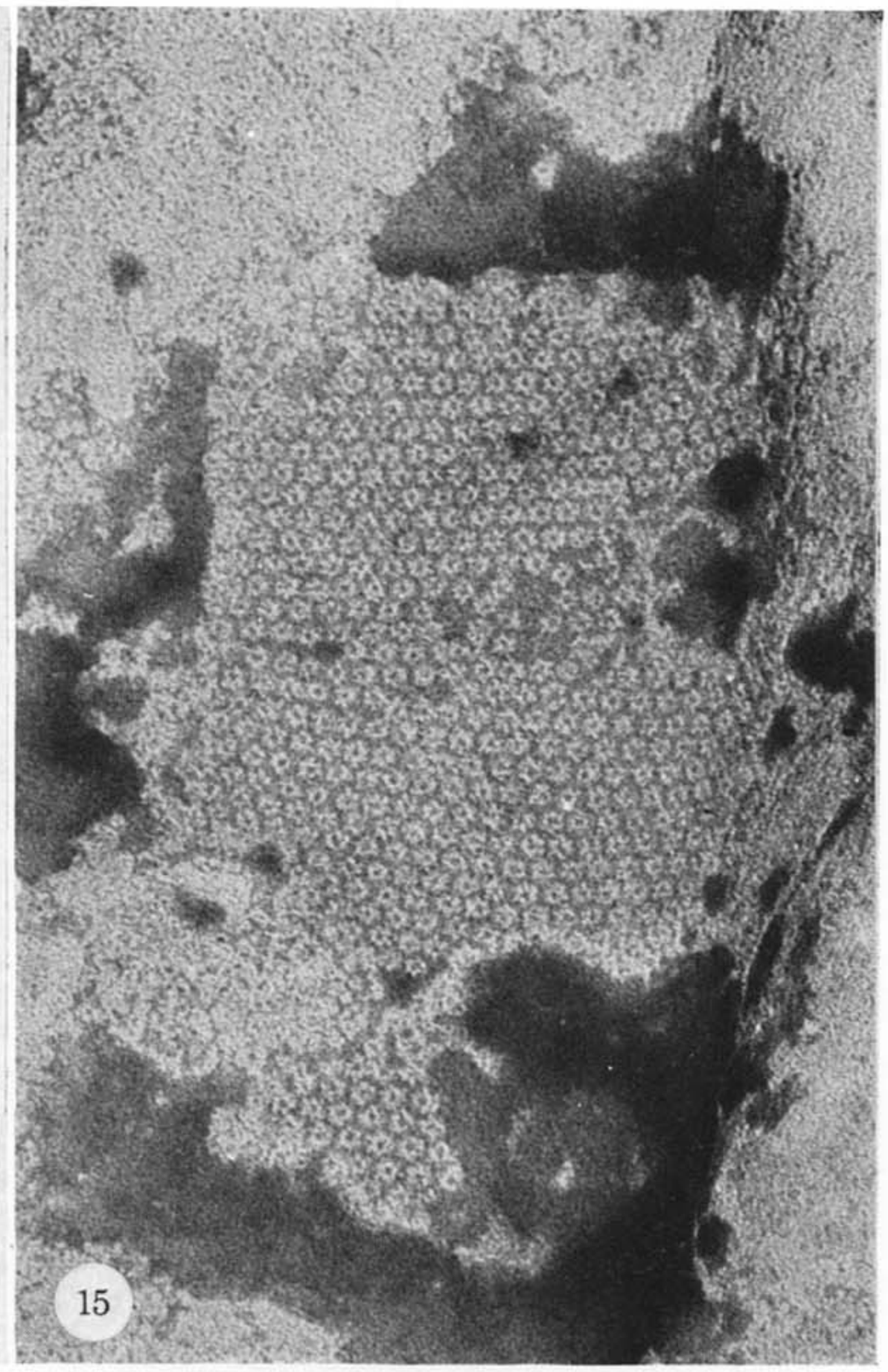

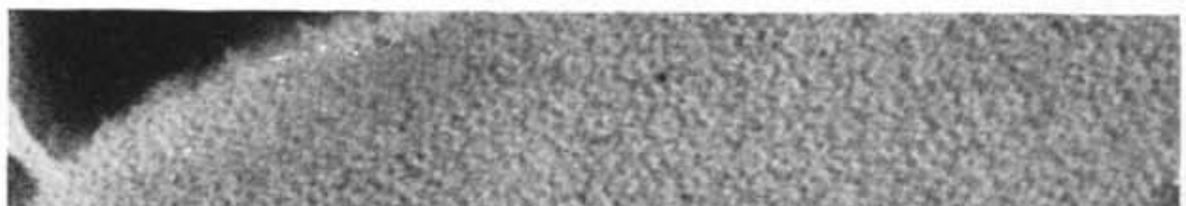

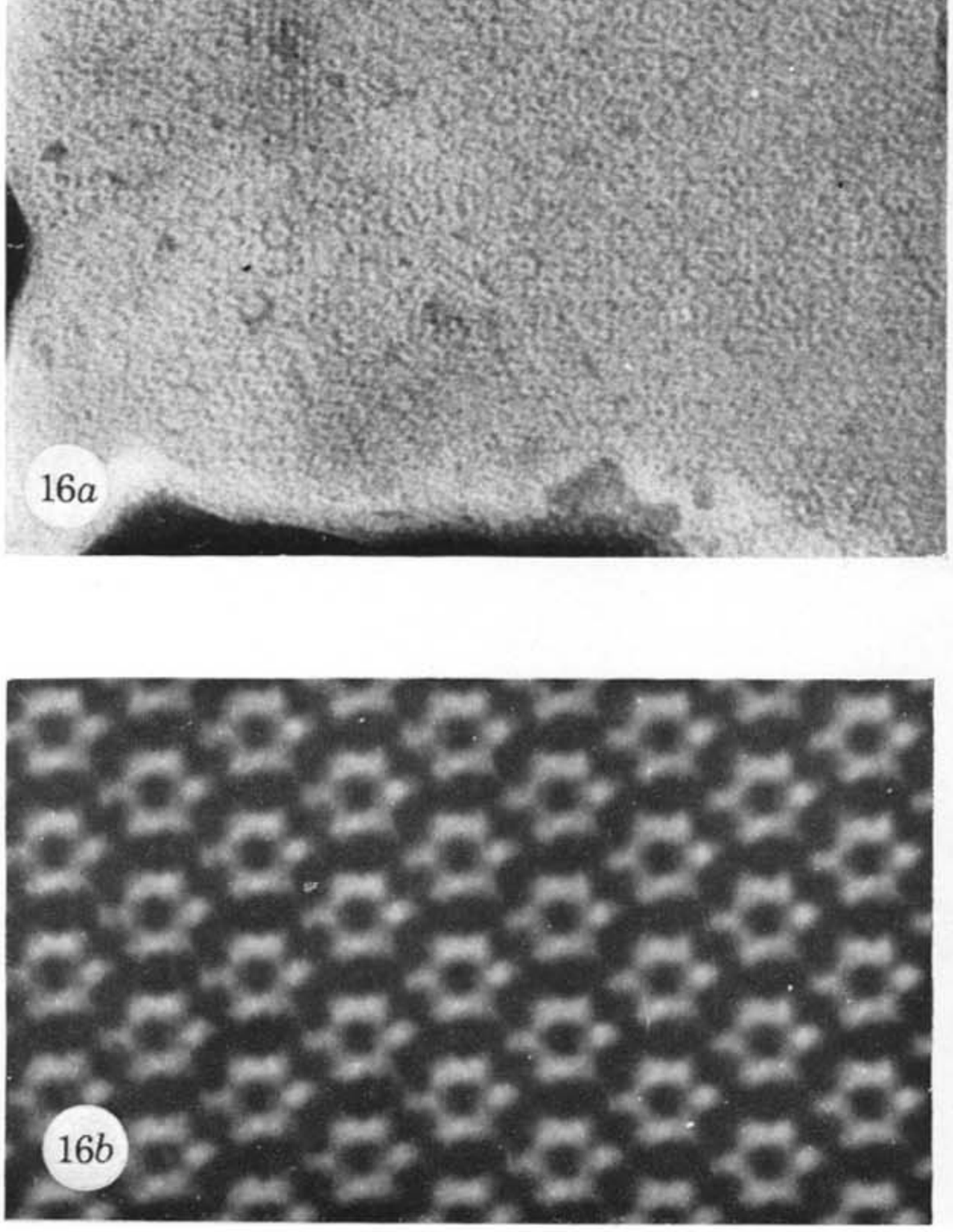

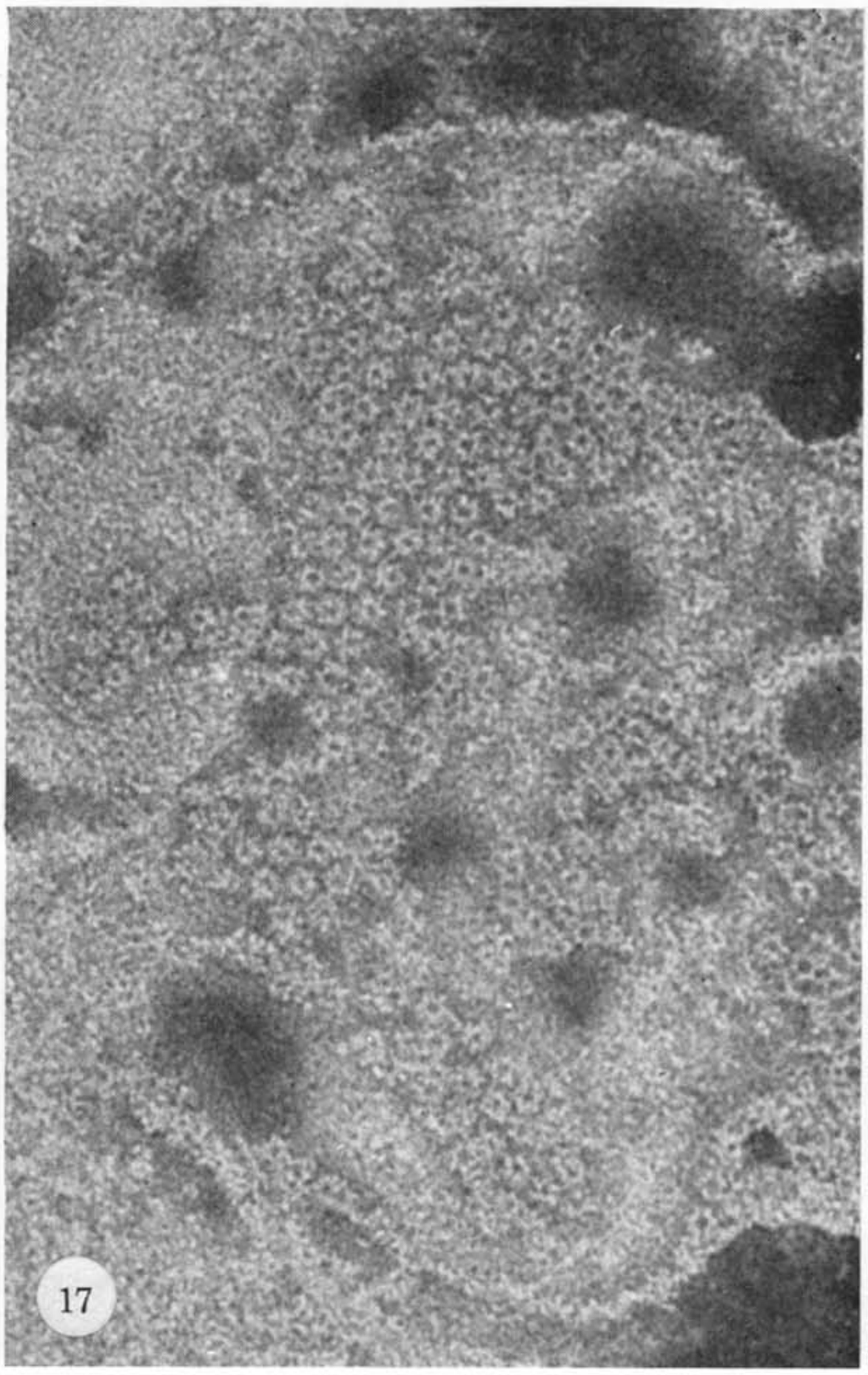

FIGURES 14–17. For description see opposite

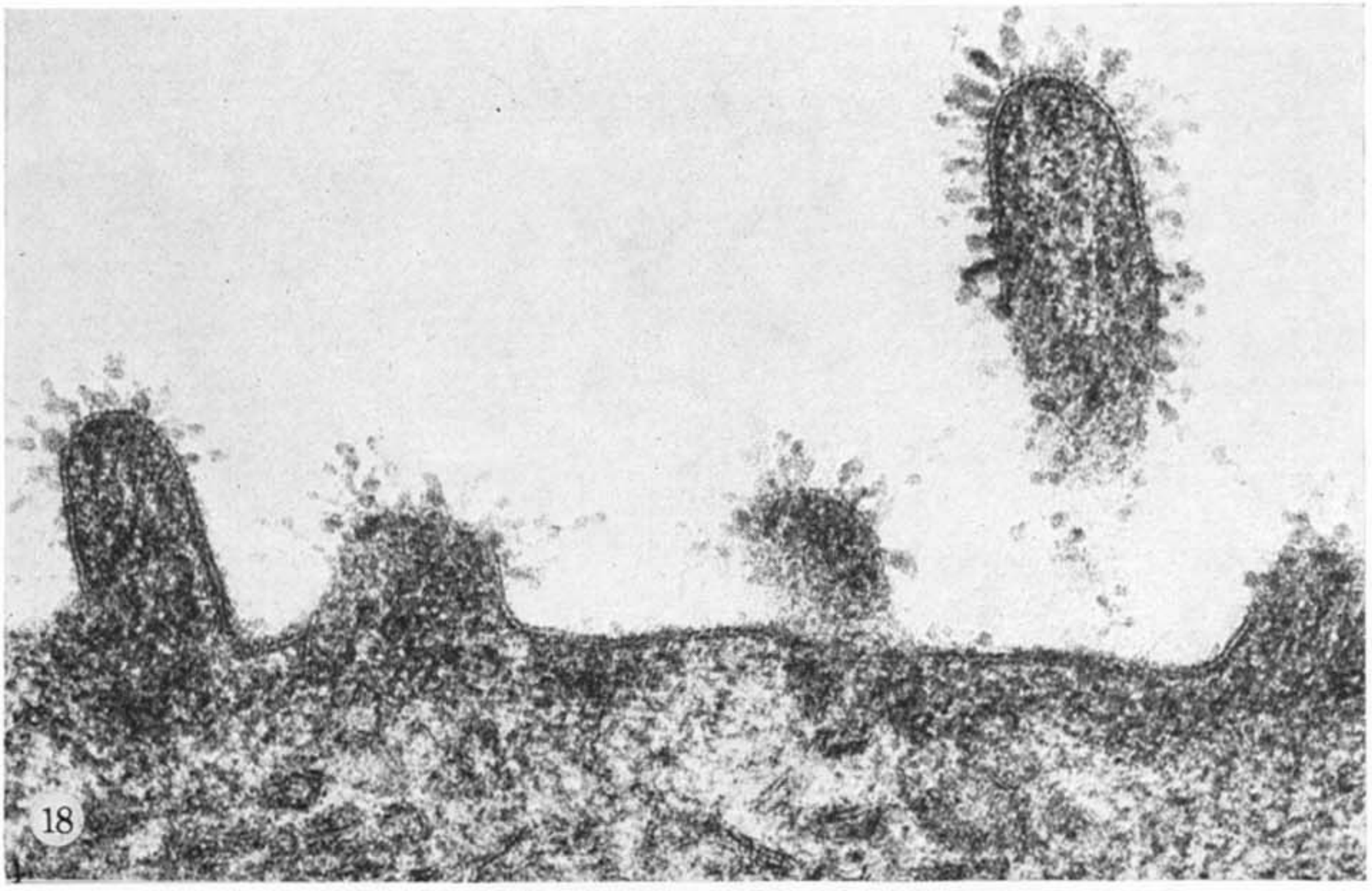

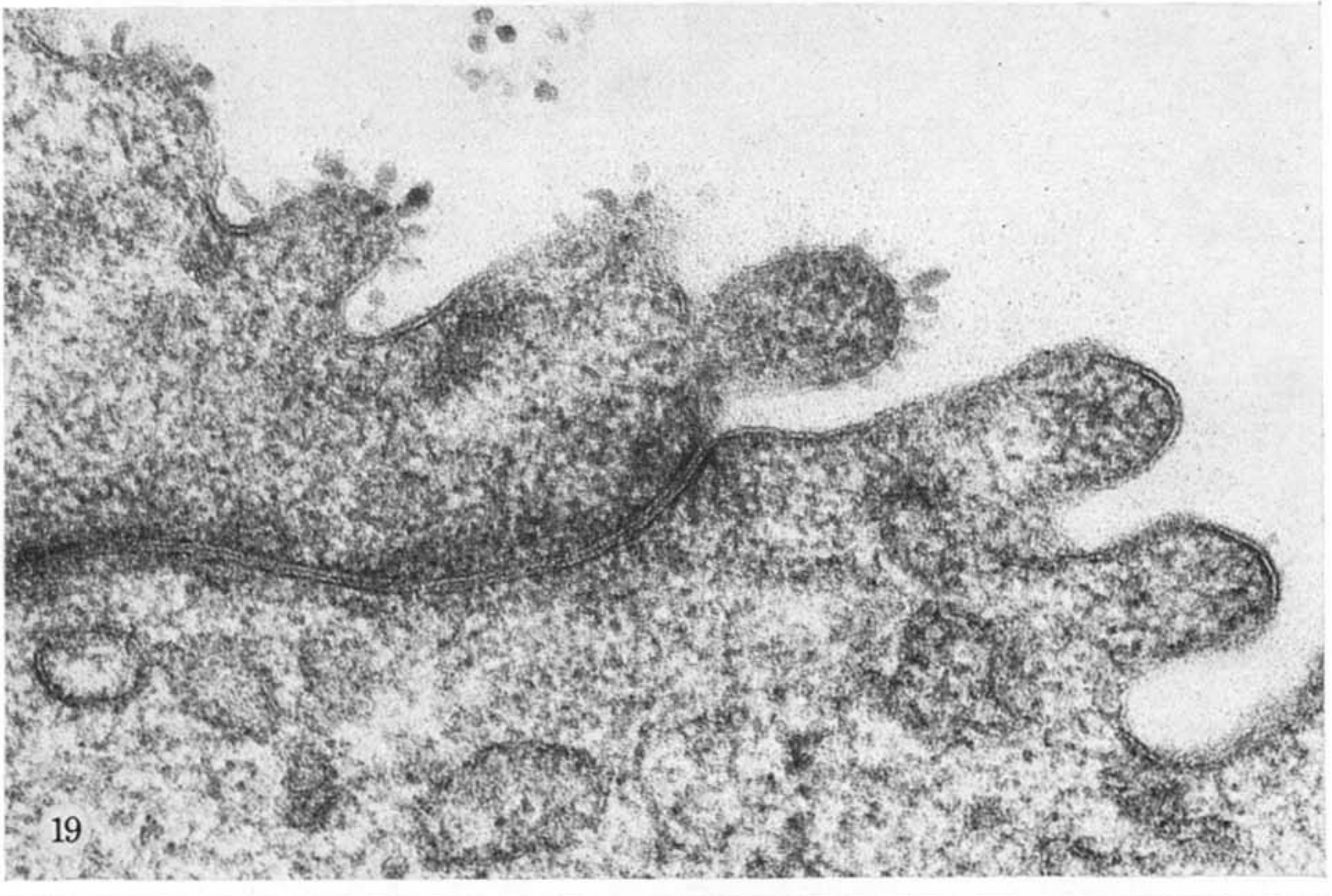

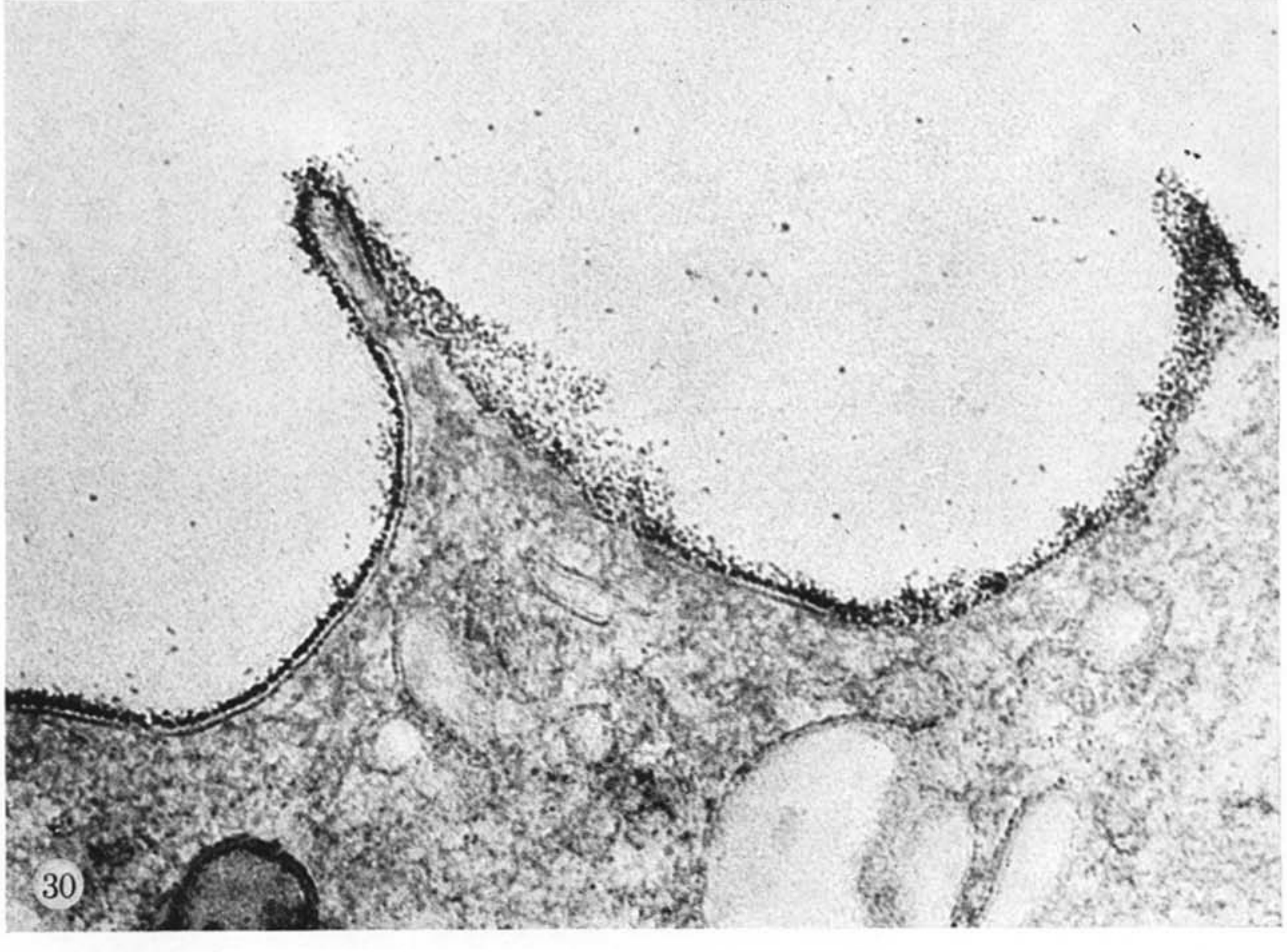

FIGURES 18–19 and 30. For description see opposite

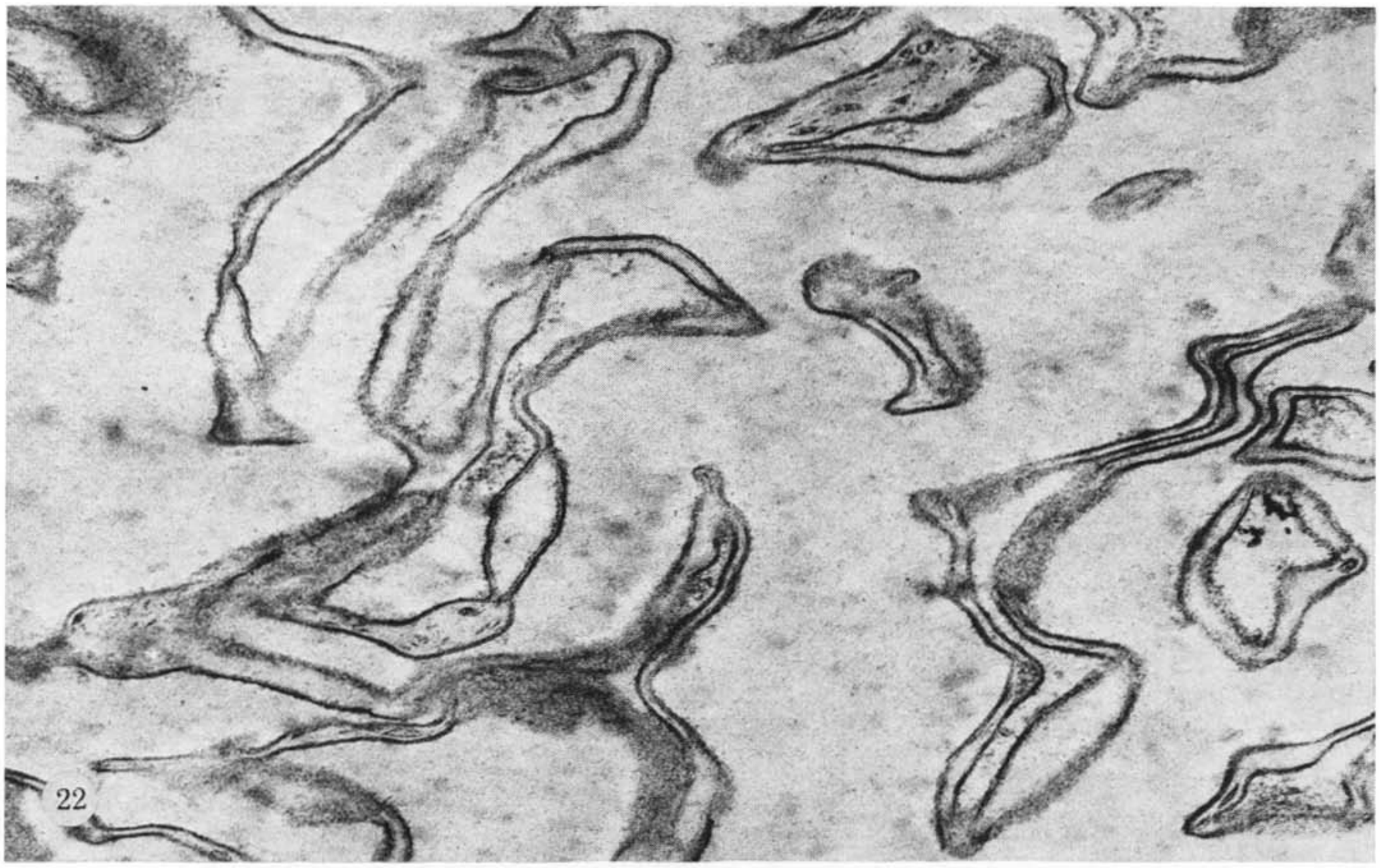

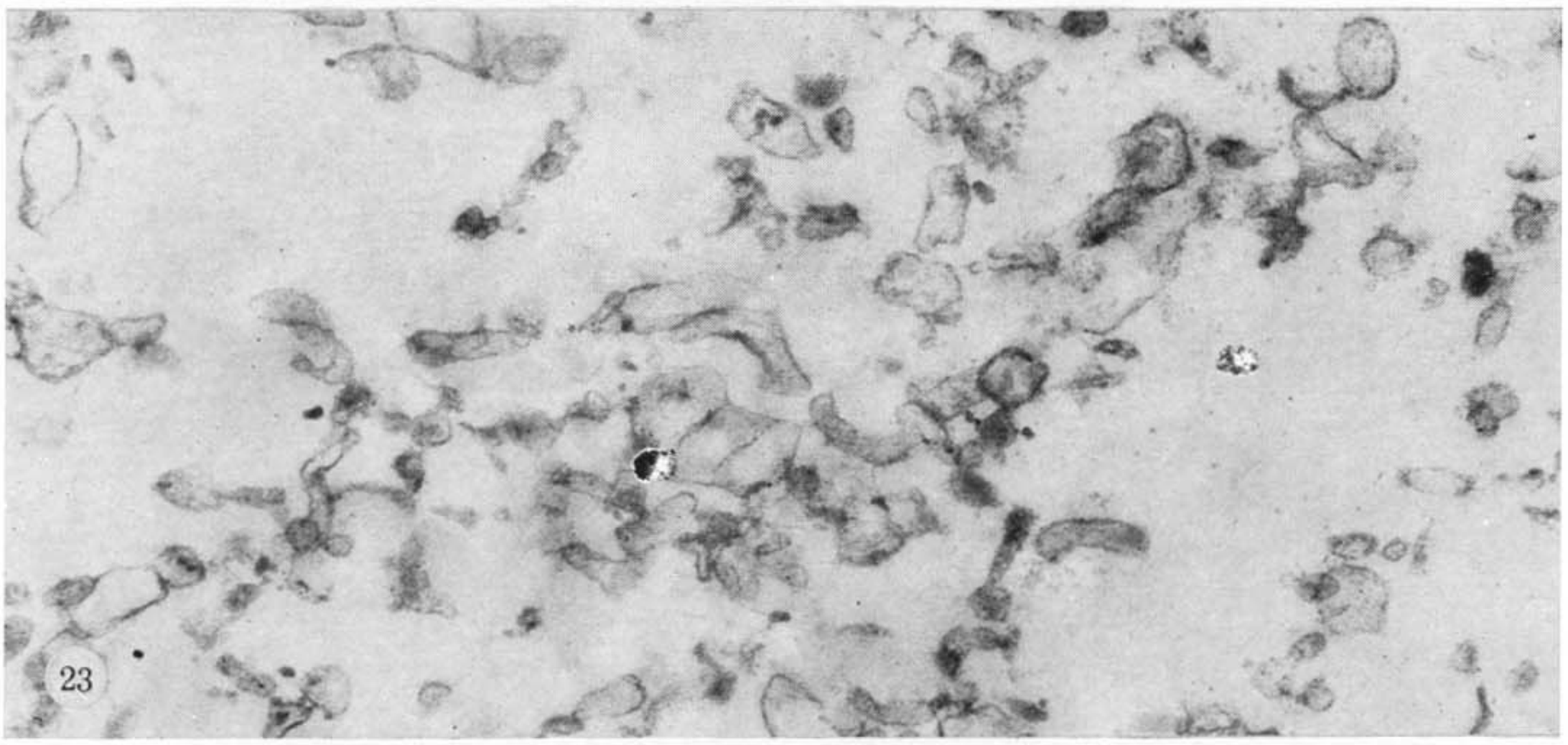

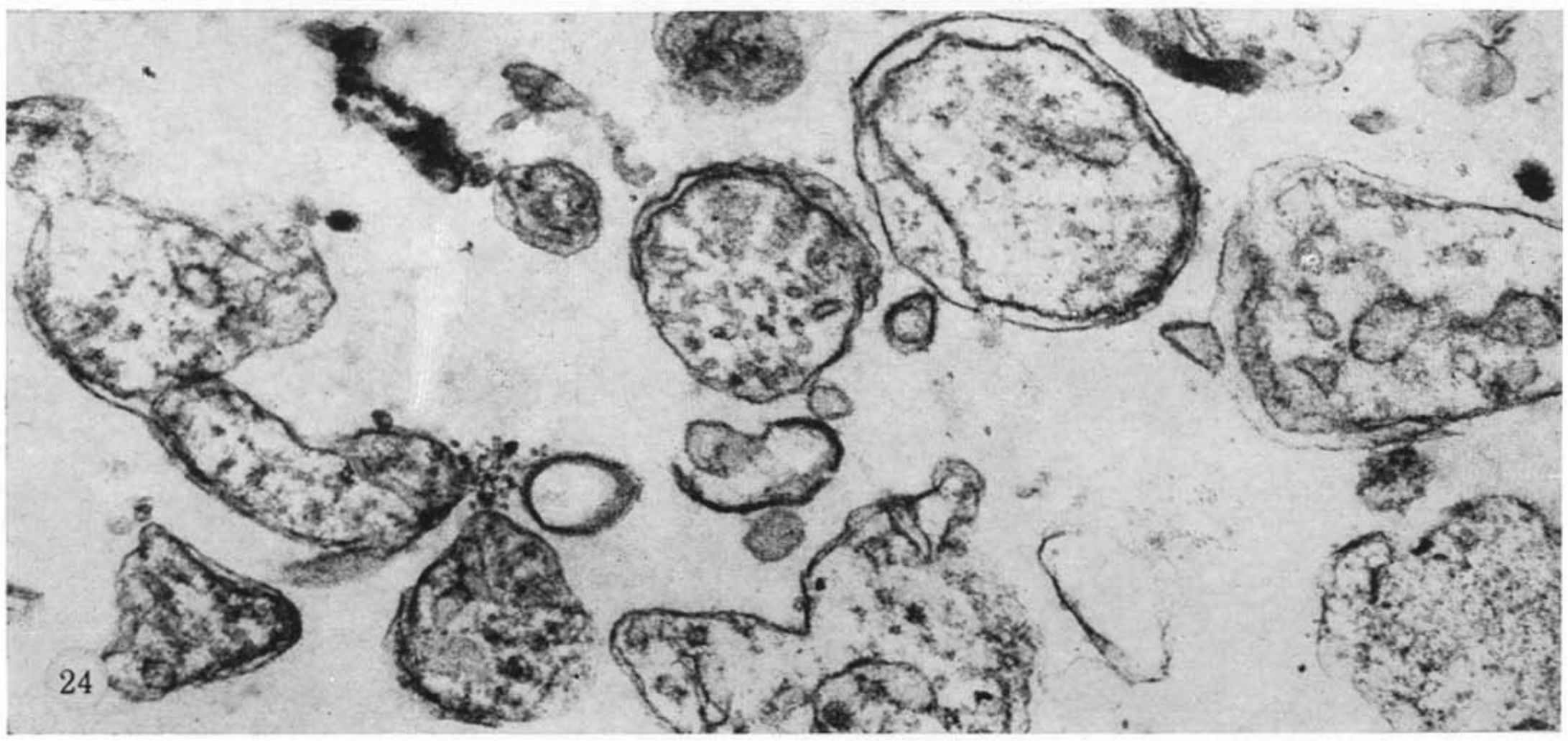

FIGURE 22. A section of pelleted bladder luminal membrane, isolated from rat bladders by the method of Hicks & Ketterer (1970). (Magn. × 50 000.)

FIGURE 23. The light membrane fraction from rat bladder, which sediments above the thick luminal membrane in the sucrose density gradient. (Magn. × 50 000.)

FIGURE 24. A part of the fraction which sediments below the luminal membrane in the density gradient. It contains mitochondria and vesicles of both thick and thin membrane. (Magn. × 50 000.)